Posttranslational Inhibition of Ty1 Retrotransposition by Nucleotide Excision Repair/Transcription Factor TFIIH Subunits Ssl2p and Rad3p

Bum-Soo Lee,* Conrad P. Lichtenstein,*,[1] Brenda Faiola,*,[2] Lori A. Rinckel,*,[3] William Wysock,*,[4] M. Joan Curcio[†] and David J. Garfinkel*

**Gene Regulation and Chromosome Biology Laboratory, Advanced BioScience Laboratories-Basic Research Program, National Cancer Institute-Frederick Cancer Research and Development Center, Frederick, Maryland 21702-1201 and [†]Molecular Genetics Program, Wadsworth Center and School of Public Health, State University of New York at Albany, Albany, New York 12201-2002*

Manuscript received September 24, 1997
Accepted for publication December 22, 1997

ABSTRACT

rtt4-1 (*r*egulator of *Ty t*ransposition) is a cellular mutation that permits a high level of spontaneous Ty1 retrotransposition in *Saccharomyces cerevisiae*. The *RTT4* gene is allelic with *SSL2* (*RAD25*), which encodes a DNA helicase present in basal transcription (TFIIH) and nucleotide excision repair (NER) complexes. The *ssl2-rtt* (*rtt4-1*) mutation stimulates Ty1 retrotransposition, but does not alter Ty1 target site preferences, or increase cDNA or mitotic recombination. In addition to *ssl2-rtt*, the *ssl2-dead* and *SSL2-1* mutations stimulate Ty1 transposition without altering the level of Ty1 RNA or proteins. However, the level of Ty1 cDNA markedly increases in the *ssl2* mutants. Like *SSL2*, certain mutations in another NER/TFIIH DNA helicase encoded by *RAD3* stimulate Ty1 transposition. Although Ssl2p and Rad3p are required for NER, inhibition of Ty1 transposition is independent of Ssl2p and Rad3p NER functions. Our work suggests that NER/TFIIH subunits antagonize Ty1 transposition posttranslationally by inhibiting reverse transcription or destabilizing Ty1 cDNA.

RETROTRANSPOSONS are a widely disseminated group of mobile genetic elements structurally and functionally related to retroviruses (for reviews, see Temin 1985; Boeke 1988; Flavell 1995). Unlike retroviruses, however, retrotransposons are not infectious. Therefore, these elements and their host genomes have evolved control systems that keep transposition at a low level (for reviews, see Garfinkel 1992; Wessler 1996), and integration site preferences that minimize insertional mutagenesis (for reviews, see Sandmeyer *et al.* 1990; Craigie 1992; Curcio and Morse 1996). The Ty element families of *Saccharomyces cerevisiae*, Ty1, Ty2, Ty3, Ty4, and Ty5, provide an excellent experimental system for understanding how retroelements and yeast coexist (for reviews, see Boeke and Sandmeyer 1991; Voytas 1996). Ty elements contain an internal coding region bracketed by two long terminal repeats (LTRs). These elements are transcribed from LTR to LTR, forming a terminally redundant transcript that is utilized as a template for both replication and translation. The internal domain contains two overlapping coding regions, *TYA* (*gag*), which encodes the nucleocapsid protein of the virus-like particle (VLP), and *TYB* (*pol*), which encodes protease (PR), integrase (IN), and reverse transcriptase/ribonuclease H (RT/RH). The TyA-TyB precursor protein is synthesized by a +1 translational frameshifting event that places *TYA* and *TYB* in the same reading frame. Linear Ty cDNA is synthesized by reverse transcription within VLPs that accumulate in the cytoplasm. Ty IN catalyzes the integration of this cDNA into new genomic sites, and the formation of a 5-base pair (bp) duplication of target DNA occurs upon insertion of the element.

Minimizing the level of Ty1 transposition is particularly important for maintaining the integrity of the yeast genome because these elements transpose, mutate essentially any yeast gene, initiate genome rearrangements, and are the most abundant Ty element family in laboratory strains. The 29 Ty1 elements present in the completely sequenced *S. cerevisiae* genome (for a review, see Goffeau *et al.* 1996) contribute as much as 0.1 to 0.8% of the total RNA present in the cell (Elder *et al.* 1983; Curcio *et al.* 1990). However, mature Ty1 proteins and VLPs are present in low levels (Garfinkel *et al.* 1985; Curcio and Garfinkel 1992), and the rate of Ty1 transposition is 10^{-5} to 10^{-7} per element per cell division (Curcio and Garfinkel 1991). The factors

Corresponding author: David J. Garfinkel, Gene Regulation and Chromosome Biology Laboratory, ABL-Basic Research Program, NCI-Frederick Cancer Research and Development Center, P.O. Box B, Frederick, MD 21702-1201. E-mail: garfinke@ncifcrf.gov

[1] *Present address:* School of Biological Sciences, Queen Mary and Westfield College, London, England E14NS.

[2] Department of Immunology, Duke University Medical Center, Durham, NC 27710.

[3] Department of Medicine, University of Maryland School of Medicine, Veterans Administration Medical Center, Baltimore, MD 21201-1524.

[4] Laboratory of Molecular Microbiology, National Institute of Allergy and Infectious Disease, NIH, Bethesda, MD 20892.

limiting Ty1 transposition have not been well characterized. Defective Ty1 elements have been hypothesized to play a major role in maintaining transpositional dormancy (Boeke *et al.* 1988). Extensive analyses of the number of transposition defective vs. competent Ty1 elements, however, suggest that most of the genomic elements are functional, and transdominant genomic Ty1 mutations do not play a major role in regulating Ty1 transposition (Curcio and Garfinkel 1994).

Even though Ty1 transposition occurs at a low level, it is greatly stimulated in cells expressing an active Ty1 element from the inducible *GAL1* promoter carried on a multicopy pGTy1 plasmid (Boeke *et al.* 1985). This growth condition is termed "transposition induction" (Garfinkel *et al.* 1985). Genetic tagging of a Ty1 element with the retrotransposition indicator gene *his3-AI* has facilitated understanding the process of retrotransposition because it allows the fate of individual genomic Ty1*his3-AI* elements to be followed (Curcio and Garfinkel 1991). The *his3-AI* gene has also been used to define a Ty1 cDNA recombination pathway that may be in competition with the transpositional integration pathway (Sharon *et al.* 1994).

TFIIH is a complex RNA polymerase II general transcription factor that has multiple roles in the cell (for reviews, see Orphanides *et al.* 1996; Svejstrup *et al.* 1996). TFIIH is required *in vitro* for transcription initiation, and promoter clearance, a step during or shortly after initiation of transcription when the RNA Pol II initiation complex is converted into an elongation complex. In addition to their essential role in transcription, certain TFIIH proteins are also required for nucleotide excision repair (NER) of damaged DNA. Yeast holo-TFIIH can be dissociated into three components: core-TFIIH which includes Rad3p and several other proteins, TFIIK which contains three proteins and has protein kinase activity, and Ssl2p (Rad25p) (Svejstrup *et al.* 1995; Guzder *et al.* 1996; Sung *et al.* 1996). Ssl2p and Rad3p are DNA helicases with opposite polarities; Ssl2p has 3′-5′ helicase activity and Rad3p has 5′-3′ helicase activity (Sung *et al.* 1987; Guzder *et al.* 1994b; Sung *et al.* 1996). NER apparently requires core TFIIH proteins, Ssl2p, but not TFIIK. Instead, core TFIIH-Ssl2 proteins become associated with gene products known to be required for NER in yeast, including those encoded by *RAD1*, *RAD2*, *RAD4*, *RAD10*, and *RAD14* (Svejstrup *et al.* 1995; Sung *et al.* 1996). The human homologs of *SSL2* and *RAD3*, *XPB/ERCC-3* and *XPD/ERCC-2*, respectively, have been found to be mutated in patients with xeroderma pigmentosum (XP), Cockayne's syndrome, and trichothiodystrophy (for a review, see Lehmann 1995). Mutations in *haywire*, the Drosophila homolog of *SSL2-XPB-ERCC3*, mimic some of the effects of XP, including ultraviolet (UV) sensitivity and neurological abnormalities (Mounkes *et al.* 1992).

SSL2, *RAD3*, as well as additional gene products comprising NER/TFIIH may have other roles in the cell. Certain mutations in *SSL1* and *SSL2* are dominant suppressors of *his4-316*, a mutation caused by a stable stem-loop structure in the 5′ leader of *HIS4* that prevents translation initiation (Gulyas and Donahue 1992; Wang *et al.* 1995). Special alleles of *RAD3* have been characterized that cause elevated mutation and recombination rates (Montelone *et al.* 1988; Song *et al.* 1990; Bailis *et al.* 1995). Interestingly, the *rad3-G595R* mutation specifically increases recombination rates between repeated sequences of 250–300 bp or less and stabilizes the ends of DNA double strand breaks (Bailis *et al.* 1995; Bailis and Maines 1996).

Previous work suggests that Ty1 transposition is regulated posttranslationally by gene products that inhibit VLP formation or function (for a review, see Farabaugh 1995). Here, we describe the characteristics of a potent *rtt* mutation (*r*egulator of *T*y *t*ransposition), *rtt4-1* (*ssl2-rtt*), which is an allele of the NER/TFIIH subunit gene *SSL2* (*RAD25*) (Gulyas and Donahue 1992; Wang *et al.* 1994). Mutations in another NER/TFIIH component, *RAD3* (Guzder *et al.* 1994a; Wang *et al.* 1994), also stimulate Ty1 transposition. Our results suggest that Ssl2p and Rad3p inhibit Ty1 transposition by preventing the accumulation of Ty1 cDNA.

MATERIALS AND METHODS

Yeast strains, media, and genetic techniques: The parental strains for mutagenesis, JC297 and JC358, were derived from GRF167 (Boeke *et al.* 1985) and GRY340 (kindly provided by J. Strathern, ABL-Basic Research Program). JC297 was isolated following induction of transposition using pGTy1-H3*his3-AI* (Curcio and Garfinkel 1991) in GRF167 and contains a single unspliced chromosomal element, designated Ty1-270*his3-AI*. The *MAT***a***::URA3* strain JC358 was derived from a cross between JC297 and GRY340, which contains a *URA3* gene integrated between the *MAT***a** and *cry1* loci. Suitable ascospores from this cross were backcrossed two additional times with JC297 to generate JC358. JC297 and JC358 and derivatives thereof contain a genomic Ty1::*lacZ* fusion in which the *E. coli lacZ* gene is fused in-frame to Ty1 IN coding sequences. Mutant *rtt4-1/ssl2-rtt* (the mutation was renamed *ssl2-rtt* after gene identification) strains DG1501 and DG1502 were derived by three backcrosses between the original *rtt4-1* isolate (JC358-6-24B) and the parental strains JC297 or JC358. DG1626 was constructed by integrating *Age*I-digested *SSL2*/YIp5 at the *SSL2* locus in JC364. The structure of the integration event at the *RTT4/SSL2* locus in DG1626 was verified by Southern analysis using ^{32}P-labeled pBR322 and *SSL2* probes. DG1722 is an isogenic *ssl2-rtt* derivative of the *SSL2* strain GRF167 constructed by two-step gene transplacement with *ssl2-rtt*/pRS406. DG1772 was constructed by gene disrupting *SSL2* with p1586 (*ssl2::TRP1*) in the presence of *SSL2*/pRS416. DG1775 (*ssl2-rtt*), DG1776 (*ssl2-dead*), DG1777 (*ssl2-x/p*), and DG1778 (*SSL2-1*) were created by plasmid shuffle as described by Gulyas and Donahue (1992). DG1751 (*ssl2-rtt*) contains the inverted repeat *ade2-5′Δ-TRP1-ade2-n* integrated at the *HIS3* locus and the *ssl2-rtt* mutation. This strain was constructed by crossing DG1722 (*ssl2-rtt*) with yAR71 (*ade2-5′Δ-TRP1-ade2-n*) and choosing a representative ascospore with the required genotype. yAR71 was kindly provided by A. Rattray (Rattray and Symington 1994). A *ssl2-rtt* derivative (DG1758)

of GRY1658 (*MAT*α-*inc::MUSH 21/18*; generously provided by J. Strathern) containing a heteroallelic *trp1* inverted repeat was constructed by two-step gene transplacement using *Age* I-cleaved *ssl2-rtt*/pRS406. BLY14, BLY15, and BLY18 were derived from DG1657 carrying pBM6 by replacing the genomic *RAD3* locus with *LEU2* by microhomologous recombination (Manivasakam *et al.* 1995), followed by plasmid shuffle with pRS414 plasmids carrying wild-type *RAD3*, *rad3-rtta*, and *rad3-rttb*, respectively. To replace the chromosomal *RAD3* locus with the *LEU2* gene by microhomologous recombination, two oligonucleotide primers, 357 and 358, were used to amplify the *LEU2* gene from plasmid pBDG874. Primer 357 is a 59-mer oligonucleotide containing 39 nucleotides homologous with nucleotides present on the 5′ end of the *RAD3* open reading frame followed by 20 nucleotides homologous with the 5′ untranslated region (UTR) of *LEU2*. Primer 358 is a 61-mer oligonucleotide containing 39 nucleotides homologous with nucleotides present on the 3′ end of the *RAD3* open reading frame followed by 21 nucleotides homologous with the 3′ UTR of *LEU2*. The PCR product containing the *LEU2* gene bracketed by sequences homologous with the 5′ and 3′ ends of *RAD3* was introduced into competent DG1657 cells carrying plasmid pBM6 to generate BLY12 containing the chromosomal *rad3::LEU2* disruption. DG1653 (*rad25-799am*) was derived from JC297 by two-step gene transplacement using plasmid pEP22 as described by Park *et al.* (1992). Congenic strains containing *rad3-2* or *RAD3*, and Ty1-270*his3-AI* were created by multiple backcrosses between RM145-3D (kindly provided by R. Malone, University of Iowa) and JC358, or JC364. The universal gene blaster technique (Alani *et al.* 1987) was used to introduce null mutations at the *ADE2*, *LEU2*, *RAD52*, or *TRP1* loci in appropriate strains. All gene transplacements were verified by complementation or Southern analyses. Other strains are listed in Table 1 and described in the text. Media were prepared as described by Sherman *et al.* (1986), Boeke *et al.* (1984), and Aguilera (1994). Certain dominance tests for the Rtt phenotype were performed in *MAT*α/α diploids to eliminate *MAT***a**/α repression of Ty1 transcription. *MAT*α/α strains were constructed by plating *MAT***a**::*URA3*/α strains on 5-fluoroorotic acid (5-FOA) medium and analyzing resistant colonies for their mating type. Sensitivity to UV radiation was determined as described by Gulyas and Donahue (1992). Standard techniques for genetic analysis, such as tetrad dissection, gene transplacements, gap-repair transformation, and plasmid shuffle were used as described by Sherman *et al.* (1986), or Guthrie and Fink (1991).

Plasmids: Plasmids were constructed by standard procedures (Sambrook *et al.* 1989). Vectors pRS406, pRS414, and pRS416 were kindly provided by R. Sikorski (Sikorski and Hieter 1989). Plasmids *SSL2*/pRS416, *ssl2-rtt*/pRS416, *SSL2*/YIp5, and *ssl2-rtt*/pRS406 were constructed by subcloning a 4594-bp *Eco*RI-*Hin*dIII fragment containing *SSL2* or *ssl2-rtt* from pCL59 or pBDG824, respectively, into the *URA3*-based centromere plasmid pRS416 or *URA3*-based integrating plasmids YIp5 (Struhl *et al.* 1979) or pRS406. Plasmid *ssl2-Age*I-fi/pRS416 was constructed by digesting *SSL2*/pRS416 with *Age*I, followed by fill-in synthesis with the Klenow fragment of DNA Polymerase I (New England Biolabs, Beverly, MA) and ligation with T4 DNA ligase (New England Biolabs). Plasmid *RAD3*/pRS414 was constructed by subcloning a 3592-bp *Sal*I-*Kpn*I fragment containing *RAD3* from p1772 (kindly provided by T. Donahue, Indiana University) into the *TRP1*-based centromere plasmid pRS414. Plasmid pBM6 (kindly provided by B. Montelone, Kansas State University) carries the *RAD3* gene in the *URA3*-based centromere plasmid YCplac33. The riboprobe plasmids pBDG689-*ACT1*, pBTB146-*LYS2*, and pBDG512-18S rDNA were constructed by subcloning a *Bam*HI-*Eco*RI fragment containing *ACT1* from pCEN-*ACT1* (kindly provided by T. Dunn, Johns Hopkins University) into pBluescript KS (+), and *Eco*RI-*Hin*dIII fragment containing *LYS2* from pSL42-2 (kindly provided by G. Fink, Whitehead Institute) into pSP70 (Promega, Madison, WI), and an *Eco*RI-*Hin*dIII fragment containing *RDN1* 18S rDNA from pRibH15 (kindly provided by A. Hinnebusch, National Institutes of Health) into pSP71 (Promega), respectively. Plasmids p1517 (*ssl2-dead*/YCp50), p1533 (*SSL2*/*LEU2-CEN4*), p1535 (*SSL2-1*/*LEU2-CEN4*), p1573 (*ssl2-x*/*p*/YCp50), and p1586 (*ssl2::TRP1* disruption) were kindly provided by T. Donahue (Gulyas and Donahue 1992), and pEP22 (*rad25-799am*/YIp5) was kindly provided by L. Prakash (Park *et al.* 1992). In collaboration with M. Jazwinski (Louisiana State University), pOY1 was constructed by subcloning an *Aat*II-*Bst*EII fragment from phis4-912 (kindly provided by G. Fink) into pBDG604, replacing the *GAL1* promoter and 5′ end of Ty1-H3*his3-AI* in YCp50 with homologous sequences from the 5′ end of Ty1-912. Plasmids pBDG456-Ty1, pBJC42-*his3-AI*, and pGTy1-H3*his3-AI* have been described previously (Curcio *et al.* 1990; Curcio and Garfinkel 1991).

Isolation of *rtt4-1*/*ssl2-rrt*: Ethylmethane sulfonate mutagenesis was performed with JC297 and JC358 as described by Sherman *et al.* (1986). Cell viability ranged between 20 and 70%. Mutagenized cells were plated on YPD plates at a density of about 300 colony-forming units per plate. The plates were incubated at 20° for 5 days and then replica plated to SC-His plates. After 3 days incubated at 30°, the number of His^+ papillae from each colony was determined. Most colonies showed ≤1 His^+ papilla per colony, which is similar to that of the parental strains. Strain JC358-6-24B (*rtt4-1*/*ssL2-rtt*) gave rise to ≥10 His^+ papillae per colony and was studied further.

Isolation of *RTT4*/*SSL2*: The wild-type *RTT4* gene was isolated by complementation of the recessive formamide-sensitivity conferred by *rtt4-1* using a YCp50-based library (Rose *et al.* 1987). Candidate transformants were tested for Ty1-270*his3-AI* transposition and growth at 37°, which are also recessive traits caused by *rtt4-1*. The insert junctions from two plasmids isolated from independent Rtt^+ transformants were sequenced using pBR322 primers (New England Biolabs) that flank the *Bam*HI cloning site of YCp50. To obtain the *rtt4-1*/*ssl2-rtt* mutation, plasmid *SSL2*/pRS416 was digested by *Bgl*II and *Blp*I, which each cleave the plasmid once outside of the *SSl2* coding region, to generate a plasmid fragment containing 128-bp and 635-bp of homologous sequences flanking the 5′ and 3′ ends of *SSL2* coding sequence, respectively. The purified plasmid fragment was used to gap-repair the *rtt4-1*/*ssL2-rtt* mutation from DG1501 after transformation. The *ssl2-rtt* mutation was identified by DNA sequencing.

Isolation of *rad3-rtt* alleles: To isolate *rad3-rtt* mutations, *RAD3*/pRS414 was mutagenized *in vitro* with hydroxylamine as described (Rose *et al.* 1990), and introduced into BLY12. Trp^+ transformants were replica plated to SC-Trp media containing 5-FOA followed by incubation at 20° for several days. The resulting colonies were replica plated to YPD medium, incubated at 20° for 6 days, and replica plated to SC-His plates. Ty1*HIS3* transposition events were scored after incubation of the SC-His plates at 25° for 4 days. Colony prints containing ≥5 His^+ papillae were retested. Mutant plasmids were rescued from each transformant and reintroduced into BLY12. BLY15 and BLY18 carrying *rad3-rtta*/pRS414 and *rad3-rttb*/pRS414, respectively, were obtained from BLY12 by plasmid shuffle, and had Rtt^- phenotypes equivalent to that of the original mutants.

Transposition assays: For qualitative estimates of spontaneous Ty1*his3-AI* transposition, cells were either spread in 2 × 2-cm patches or streaked for single colonies on YPD plates and incubated at 20° for 5 days. The plates were then replica plated

TABLE 1

List of yeast strains

Strain name	Genotype	Source[a]
JC297	*MAT*α *ura3-167 his3-*Δ*200 trp1-hisG* Ty1-270*his3-AI* Ty1-588*neo* Ty*1-146*[*tyb1::lacZ*]	
JC358	*MAT***a***::URA3 ura3 ade2-101 his3-*Δ*200* Ty1-270*his3-AI* Ty1-588*neo* Ty1-146[*tyb1::lacZ*]	
JC358-6-24B	JC358 *rtt4-1/ssl2-rtt*	
JC364	*MAT***a** *ura3-167 his3-*Δ*200 leu2-hisG* Ty1-270*his3-AI* Ty1-588*neo* Ty1-146[*tyb1::lacZ*]	
GRF167	*MAT*α *ura3-167 his3-*Δ*200 GAL*	Boeke *et al.* 1985
JJ565	*MAT***a** *ura3-52 his4-316 ino1-13*	Gulyas and Donahue 1992
JJ586	*MAT***a** *ura3-52 his4-316 ino1-13 SSL2-1*	Gulyas and Donahue 1992
GRY340	*MAT***a***::URA3 ura3-52 his3-*Δ*200 ade2-101 cry1 trp1-*Δ*1 leu2-*Δ*1 lys2-801*	J. Strathern
GRY1658	*MAT*α*::MUSH21/18 can1-*Δ*1 lys2-hisG tyr7-1 ura3-52 his3-*Δ*200 leu2-*Δ*1 trp1-hisG*	J. Strathern
yAR71	*MAT***a** *ade2-hisG::URA3 can1-100 ade2-5′*Δ*-TRP1-ade2-n leu2-3,2-112 trp1-1 ura3-1*	Rattray and Symington 1994
RM145-3D	*MAT*α *rad3-2 leu2-3,2-112 can1 ura3-13 ade5 met13-d ade2-1*	R. Malone
BLY12	DG1657 *rad3::LEU2* (pBM6)	
BLY14	DG1657 *rad3::LEU2* (*RAD3*/pRS414)	
BLY15	DG1657 *rad3::LEU2* (*rad3-rtta*/pRS414)	
BLY18	DG1657 *rad3::LEU2* (*rad3-rttb*/pRS414)	
S288c	*MAT*α	G. Fink
DG789	GRF167 *spt3-101*	Curcio and Garfinkel 1991
DG1044	*mat*Δ*::URA3 his3-*Δ*1 leu2-3,2-112 trp1-289 ura3 can1 GAL*	
DG1501	*MAT*α *ura3-167 ssl2-rtt his3-*Δ*200* Ty1-270*his3-AI* Ty1-588*neo* Ty1-146[*tyb1::lacZ*]	
DG1502	*MAT***a***::URA3 ura3 ade2-101 ssl2-rtt his3-*Δ*200* Tyl-270*his3-AI* Ty1-588*neo* Ty1-146[*tyb1::lacZ*]	
DG1520	JC364 *rad52-hisG::URA3*	
DG1626	JC364 *SSL2::SSL2*/YIp5	
DG1636	*MAT***a** *ura3-167 rad52-hisG::URA3 his3-*Δ*200* Ty1-270*his3-AI* Ty1-588*neo* Ty1-146[*tyb1::lacZ*]	
DG1637	*MAT***a** *ura3-167 ssl2-rtt his3-*Δ*200* Ty1-270*his3-AI* Ty1-588*neo* Ty1-146[*tyb1::lacZ*]	
DG1638	*MAT***a** *ura3-167 rad52-hisG::URA3 ssl2-rtt his3-*Δ*200* Ty1-270*his3-AI* Ty1-588*neo* Ty1-146[*tyb1::lacZ*]	
DG1639	*MAT***a** *ura3-167 his3-*Δ*200* Ty1-270*his3-AI* Ty1-588*neo* Ty1-146[*tyb1::lacZ*]	
DG1653	JC297 *rad25-799am*	
DG1657	*MAT***a** *ura3-167 his3-*Δ*200 trp1-hisG leu2-hisG* Ty1-270*his3-AI* Ty1-588*neo* Ty1-146[*tyb1::lacZ*]	
DG1721	DG1722 (pOY1)	
DG1722	GRF167 *ssl2-rtt*	
DG1725	GRF167 (pOY1)	
DG1740	DG1722 (pGTy1-H3*his3-AI*)	
DG1741	GRF167 (pGTy1-H3*his3-AI*)	
DG1751	*MAT***a** *ura3 ssl2-rtt can1-100 leu2-3,2-112 ade2-5′*Δ*-TRP1-ade2-n*	
DG1758	GRY1658 *ssl2-rtt*	
DG1772	DG1657 *ssl2::TRP1 (SSL2/pRS416*)	
DG1774	DG1657 *ssl2::TRP1* (*SSL2/LEU2-CEN4*)	
DG1775	DG1657 *ss12::TRP1 (ssl2-rtt*/pRS416)	
DG1776	DG1657 *ssl2::TRP1 (ssl2-dead*/YCp50)	
DG1777	DG1657 *ssl2::TRP1* (*ssl2-x/p/*YCp50)	
DG1778	DG1657 *ssl2::TRP1* (*SSL2-1/LEU2-CEN4*)	
DG1793	JJ565 *ssl2-rtt*	

[a] All strains are from this study unless otherwise noted.

to SC-His plates and incubated at 25° or 30° for 4 days. The rate of spontaneous Ty1*his3-AI* transposition was determined as described by Curcio and Garfinkel (1991), except that median frequencies were converted to rates according to the method of Drake (1970). The rate of spontaneous Ty-induced *can1* mutations was obtained by multiplying the mutation rate to *can1* by the fraction of mutations caused by Ty insertion. The *can1* mutation rate resulting from non-Ty events was determined by multiplying the *can1* mutation rate by the fraction of mutants not caused by Ty insertion. The mutation rate to *can1* was determined according to the method of Drake (1970). The position of Ty insertions at *CAN1* was determined as described by Rinckel and Garfinkel (1996). The efficiency of pGTy1-H3*his3-AI* transposition was determined as described by Curcio and Garfinkel (1991). Spontaneous transposition events upstream of glycine tRNA genes were detected after individual colonies were grown on YPD plates for 7 days at 20°. Six colonies were then individually inoculated into 10 ml of YPD and grown for an additional two days at 20°. Total DNA isolated from these cultures was analyzed by PCR using

primers specific for the target site and Ty1 and Ty2. A glycine tRNA-specific primer *SUF16* OUT, 5′GGATTTTACCACTAAA CCACTT3′, was chosen to detect Ty insertions upstream of glycine tRNA genes, and is located within the glycine tRNA transcription unit. The Ty-specific primer AX020, 5′CTATTA CATTATGGGTGGTATG3′, is near the Ty1 and Ty2 element's polypurine tract just inside of the 3′ LTR. The *SUF16* OUT oligonucleotide was 5′-end labeled using T4 polynucleotide kinase (New England Biolabs) and [γ-^{32}P]-ATP (Amersham, Arlington Heights, IL). PCR was performed using the following conditions: 10 cycles at 94°, 30 sec; 67°, 30 sec; 72°, 1 min followed by 20 cycles at 94°, 30 sec; 62°, 30 sec; 72°, 1 min. A portion of the reaction was separated by agarose gel electrophoresis on a 2% (w/v) gel. The gel was dried at 50° under vacuum, then autoradiographed. Control PCR amplifications using *TRP1*-specific primers were performed to insure that the DNA samples were PCR-competent.

Mitotic recombination: Intrachromosomal mitotic recombination assays developed by Rattray and Symington (1994), and J. Strathern (personal communication) were utilized essentially as described (Rattray and Symington 1994), except that Noble agar (Difco, Detroit) was used in the SC-Ade plates. Median recombination rates were calculated by the method of Drake (1970).

Northern blot analysis: Yeast strains were grown at 20° in YPD or SC-Ura media to mid-to-late log (2–3 days incubation) or stationary (5 days incubation) phase. Total RNA was isolated, separated electrophoretically, and blotted to Hybond N (Amersham) nylon membranes as described previously (Curcio *et al.* 1990). ^{32}P-labeled RNA probes were synthesized from plasmids pBDG689-*ACT1*, pBTB146-*LYS2*, pBDG512-18S rDNA, pBDG456-Ty1, and pBJC242-*his3-AI* by *in vitro* transcription (Promega). DNA probes were made by randomly primed DNA synthesis (Amersham) or 5′-end labeling using T4 polynucleotide kinase (United States Biochemical, Cleveland). A 3.6-kb *Pvu*II fragment containing Ty1 sequences from pOY1 was used to make the Ty1 hybridization probe. The Ty1-912/H3*his3-AI* and Ty1-270*his3-AI* probe was made from a 0.5-kb *Pst*I fragment containing the *his3-AI* region from pOY1. An isoleucine pre-tRNA probe was prepared by 5′-end labeling the 45 nucleotide intron of the tRNA as described previously (Qiu *et al.* 1993). Multiple probes were sometimes added to one filter, or single probes were sequentially added to the same filter after the previous probe was removed. Hybridization signals were quantitated by phosphorimage analysis using conditions suggested by the manufacturer (Molecular Dynamics, Inc., Sunnyvale, CA) and ImageQuant software (Version 1.1).

Protein analysis: Total protein extracts were prepared as described by Atkin *et al.* (1995) using a lysis buffer containing 5 mm EDTA, 250 mm NaCl, 0.1% (v/v) Nonidet P-40, 50 mm Tris-HCl (pH 7.4), 0.1 mm PMSF, and 1 μg/ml of each of the following protease inhibitors: pepstatin, leupeptin, aprotinin, antipain, and chymostatin. Endogenous VLPs from uninduced cells were fractionated by sedimentation through a sucrose step gradient as described previously (Eichinger and Boeke 1988). Typically one liter of mid-to-late log phase cells grown in YPD broth was used for isolation of endogenous VLPs. VLPs from cells expressing pGTy1-H3*his3-AI* were prepared as described previously (Eichinger and Boeke 1988). Protein concentrations were determined using commercially available reagents (BioRad Labs., Hercules, CA, or Pierce Chemical Co., Rockford, IL). Proteins separated on SDS-polyacrylamide gels were transferred to Immobilon-P membranes (Millipore, Bedford, MA) using a Bio Rad electrophoretic transfer apparatus or a semi-dry electroblotter (ISS Inc., Champaign, IL). After transfer, membrane-bound proteins were visualized with Ponceau S stain (Sigma Chemical Co., St. Louis). The polyclonal antisera to Ty1-VLPs, Ty1 IN, and Ty1 RT/RH are described in detail elsewhere (Youngren *et al.* 1988; Garfinkel *et al.* 1991). Antiserum to Hts1p was kindly provided by T. Mason (University of Massachusetts, Amherst). Immunodetection was performed using enhanced chemiluminscence (ECL) as described by the supplier (Amersham). ECL signals were quantitated by laser densitometry using an Ultroscan XL densitometer (LKB, Piscataway, NJ). Protein molecular weight standard were obtained from BioRad. Standard methods were used to prepare protein extracts from yeast and determine β-galactosidase activity (Rose *et al.* 1981). One unit is defined as one nanomole o-nitrophenyl galactoside converted per mg protein per min.

Southern blot analysis of Ty1 cDNA: A single colony of each strain inoculated into 1–2 ml of YPD broth was grown overnight at 20°. These cultures were diluted 100-fold into 20 ml YPD and grown for two days at 20°. Yeast DNA was prepared for Southern analysis as described by Hoffman and Winston (1987). For detection of Ty1 VLP-associated cDNA, cellular extracts enriched for VLPs were deproteinized with phenol and total nucleic acid was recovered as described by Garfinkel *et al.* (1985). DNA samples digested with *Pvu*II were separated by 0.8% (w/v) agarose gel electrophoresis, and capillary-blotted to Hybond N+ nylon membrane (Amersham). The resulting filter was hybridized with a randomly-primed ^{32}P-labeled Ty1-H3 *Pvu*II-*Sna*B1 fragment that spans the Ty1 RT/RH gene. Four conserved Ty1-chromosomal junction fragments were used as internal standards to normalize the level of Ty1 cDNA in each sample. Hybridization signals were quantitated by phosphorimage analysis as described above.

RESULTS

Isolation of *rtt4-1* (*ssl2-rtt*): *rtt4-1* came from a collection of 143 chromosomal mutants that display a high frequency of putative Ty1 transposition events, as monitored by the increased level of His$^+$ prototroph formation by a genomic element Ty1-270 marked with the retrotransposition indicator gene, *his3-AI* (Figure 1, A and B) (Curcio and Garfinkel 1991). The original *rtt4-1* mutant, JC358-6-24B, was temperature sensitive for growth at 37°, weakly sensitive to UV radiation, and sensitive to 3% formamide in the growth medium. JC358-6-24B was backcrossed three times to the parental strains JC297 or JC358 to generate congenic *MAT***a** and *MAT*α strains DG1502 and DG1501 (Figure 1C), respectively. The temperature and formamide sensitivities, and the Rtt$^-$ phenotype, as monitored by Ty1-270*his3-AI* His$^+$ levels, were recessive and tightly linked in each backcross. These results suggest that a single mutation is responsible for the three phenotypes. When the rate of His$^+$ formation was determined in congenic *rtt4-1* strains DG1501 and DG1502, and the *RTT4* strain JC297, the *rtt4-1* mutation caused a 400- to 1125-fold increase in Ty1-270*his3-AI* mediated His$^+$ events (Table 2A). Southern analysis of 24 independent His$^+$ events from either DG1501 or JC297 grown at 20° was performed using a ^{32}P-labeled *HIS3* probe, and each isolate contained a single Ty1*HIS3* element present at apparently novel sites (data not shown).

***rtt4-1* is an allele of *SSL2* (*RAD25*):** The results of the preceding experiments served as the basis for cloning

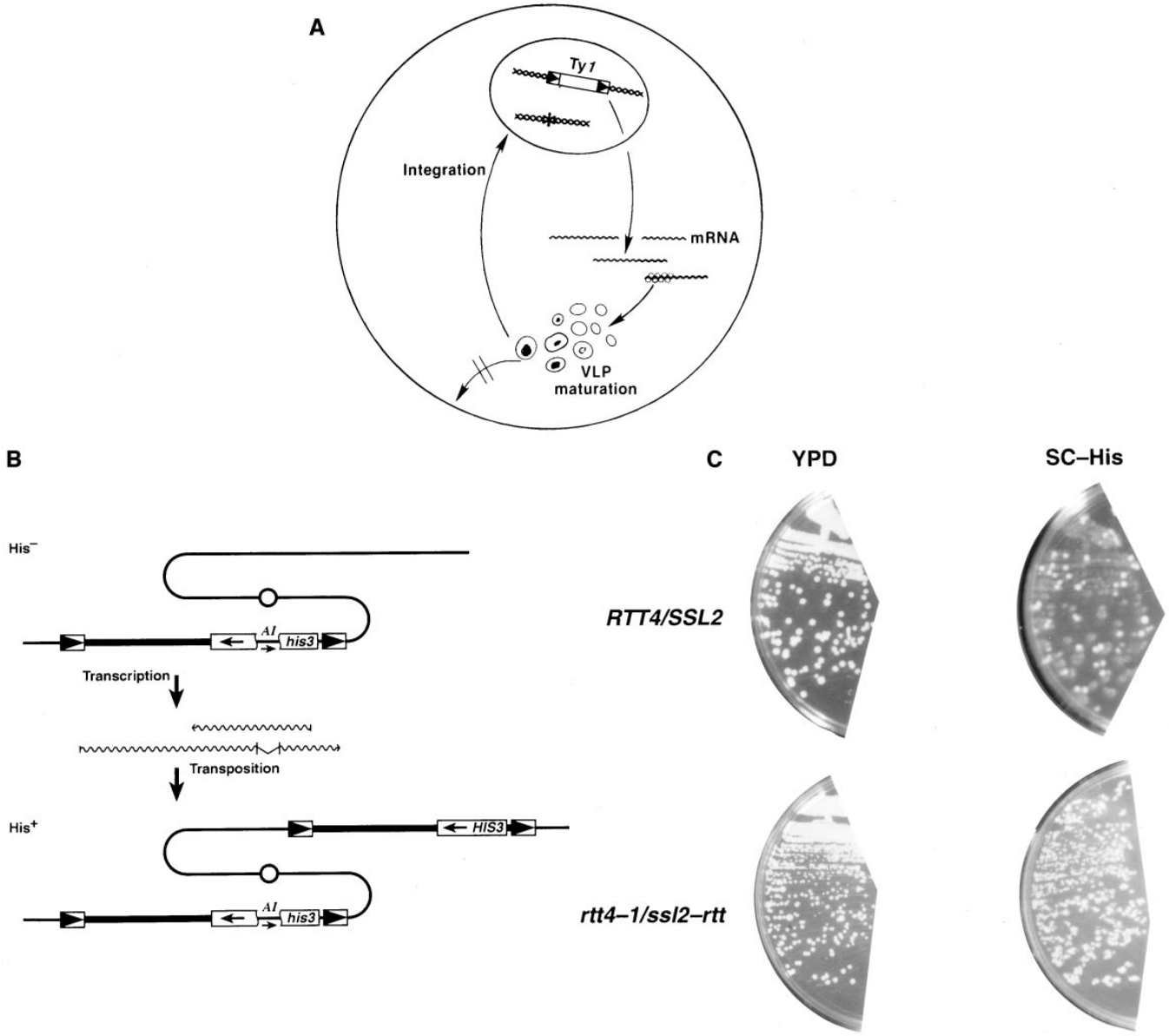

Figure 1.—Experimental system used to isolate *rtt4-1*/*ssl2-rtt*. (A) Ty1 life cycle. Ty1 elements reside in the nuclear genome where they are transcribed. Ty1 RNA is terminally redundant because directly repeated LTR (long terminal repeat) sequences present at the ends of the element are transcribed (boxed arrows point in the direction of Ty1 transcription). Ty1 RNA directs the synthesis of proteins that are essential for transposition. These include capsid proteins of the virus-like particle (VLP), and enzymes required for protein processing, reverse transcription, and integration. Ty1-VLPs do not leave the cell. A preintegration complex made up of at least integrase and Ty1 cDNA probably journeys back to the nucleus where integration takes place. (B) Phenotypic detection of transposition of a genomic Ty1 element marked with the retrotransposition indicator gene *his3-AI*. The Ty1 element is tagged at the 3′ end with *his3-AI*, which is the yeast *HIS3* gene interrupted by an artificial intron, *AI*. Boxed area represents the *HIS3* gene and its direction of transcription, opposite to that of Ty1, is shown by the enclosed arrow. *AI*, represented by the thin line, is inserted into the *HIS3* coding sequence in an antisense orientation relative to *HIS3* transcription, as indicated by the arrow below the *AI*. Cells containing *his3-AI* are phenotypically His$^-$. *AI*, however, is in the sense orientation relative to the Ty1 transcript. The Ty1 transcript is represented by the wavy line and splicing of the *AI* is indicated by vertical lines in the Ty1 transcript. When a spliced transcript undergoes retrotransposition, a new copy of the element with a functional *HIS3* gene (Ty1*HIS3*) is recreated by precise removal of the *AI*. This duplicative transposition event renders the cell phenotypically His$^+$. The transposition event is shown as occurring on the same chromosome for simplicity. (C) Increased levels of Ty1 transposition in a *rtt4-1*/*ssl2-rtt* background, as monitored by chromosomal Ty1-270*his3-AI* transposition. Parental (JC297; *RTT4*/*SSL2*) and mutant (DG1501; *rtt4-1*/*ssl2-rtt*) strains were streaked for single colonies on a YPD plate and incubated for 5 days at 20°. Spontaneous Ty1*HIS3* transposition events were detected as His$^+$ papillae by replica plating the YPD plate to SC-His medium, followed by incubation for 4 days at 25°.

TABLE 2

Transposition of Ty1*his3-AI* elements

Strain	Relevant genotype	Transposition rate[a] ($\times 10^{-6}$)	Fold-increase[b] (mutant/wild-type)
(A) DG1501	*rtt4-1/ssl2-rtt*	16	400
DG1502	*rtt4-1/ssl2-rtt*	45	1125
JC297	*RTT4/SSL2*	0.04	1
(B) DG1721	*ssl2-rtt*	90	180
DG1725	*SSL2*	0.5	1
(C) DG1520	*rad52-hisG::URA3*	0.53	6.3
JC364	*RAD52*	0.084	1
(D) DG1636	*rad52-hisG::URA3* *SSL2*	0.2	6.3
DG1637	*ssl2-rtt* *RAD52*	4.3	143
DG1638	*rad52-hisG::URA3* *ssl2-rtt*	7.5	250
DG1639	*RAD52 SSL2*	0.03	1

[a] Rate of His^+ prototroph formation per cell per generation as determined by the method of Drake (1970).
[b] Mutant transposition rate over the wild-type rate for each set of strains.

the wild-type *RTT4* gene. The *RTT4* gene was cloned from a YCp50 genomic library (Rose *et al.* 1987) by complementation of the *rtt4-1* formamide-sensitive phenotype. Candidate transformants were then tested for growth at 37° and Ty1-270*his3-AI* transposition. Plasmids were isolated from two formamide-resistant, temperature-resistant, Rtt^+ transformants that were suspected to contain the wild-type *RTT4* gene. These plasmids contained overlapping inserts, as demonstrated by restriction enzyme and DNA sequence analyses (*Saccharomyces* Genome Data Base, Stanford University). The only complete gene common to both cloned inserts was *SSL2* (also known as *RAD25*), an essential gene involved in RNA Pol II transcription and NER (Gulyas and Donahue 1992; Park *et al.* 1992; Feaver *et al.* 1993; Guzder *et al.* 1994b). A 4594-bp *Eco*RI-*Hin*dIII fragment containing *SSL2* was subcloned into the centromere plasmid pRS416 and the integrating vector YIp5. The *RTT4*/*SSL2*/pRS416 subclone complemented all mutant defects conferred by *rtt4-1*. This plasmid also complemented the severe UV-sensitivity of a previously characterized *ssl2* mutation, *rad25-799am* (Park *et al.* 1992), in strain DG1653. When a frameshift mutation was introduced into the middle of the *SSL2* coding sequence by filling in an *Age*I restriction site, the resulting *ssl2-Age*I-fi/pRS416 plasmid failed to complement *rtt4-1* and *rad25-799am*, and was recessive to wild-type *SSL2*. Crossing a *SSL2* strain (DG1626) containing a *SSL2*/YIp5 plasmid integrated at *SSL2* with a *rtt4-1* strain (DG1501) demonstrated tight linkage between *rtt4-1* and the integrated *URA3* marker present on YIp5 (16 parental ditype: 0 nonparental ditype: 0 tetratype asci). We now refer to *rtt4-1* as *ssl2-rtt*, since these results show that *rtt4-1* is an allele of *SSL2*.

The *ssl2-rtt* region was rescued from DG1501 by gap-repair recombination. The resulting plasmid showed no gross rearrangement of the *Eco*RI-*Hin*dIII insert or the plasmid backbone, as monitored by restriction enzyme analysis. The *ssl2-rtt*/pRS416 centromere plasmid failed to complement the *ssl2-rtt* mutation, and the plasmid-borne *ssl2-rtt* mutation was recessive to wild-type *SSL2* and *rad25-799am* with respect to the Rtt^- phenotype. The DNA sequence of the *Eco*RI-*Hin*dIII fragment present in the gap-repaired *ssl2-rtt*/pRS416 plasmid was determined and shown to be identical to that of *SSL2*, except for a G→A transition at codon 556, which changes glutamic acid (GAG) to lysine (AAG). This mutation was confirmed by direct sequencing of PCR-generated *SSL2* and *ssl2-rtt* alleles from our strains, and transformation experiments using PCR fragments spanning codon 556 of *SSL2* (data not shown). Codon 556 is located between the conserved helicase sequence motifs III and IV (Walker *et al.* 1982) of *SSL2*, and the glutamic acid codon at this position is conserved in human *XPB*/*ERCC-3* and Drosophila *haywire*. Surprisingly, Qiu *et al.* (1993) showed that a temperature sensitive *ssl2* allele, *rad25-ts24*, generated by *in vitro* mutagenesis with hydroxylamine, contains both a V552I mutation and the identical *ssl2-rtt* E556K mutation.

An isogenic *ssl2-rtt* derivative of GRF167, DG1722, was constructed by two-step gene transplacement using a *ssl2-rtt*/pRS406 integrating plasmid for further studies of Ty1 transposition. DG1722 and the congenic strains, DG1501 and DG1502, had similar growth characteristics. We initially examined Ty1*his3-AI* transposition (Table 2B) to determine whether this key phenotype was maintained in DG1722. Since GRF167 does not contain a genomic Ty1*his3-AI* element, a functional Ty1-912/H3*his3-AI* hybrid element present on the centromere

TABLE 3

Ty1 insertional mutagenesis of *CAN1*

Strain	Relevant genotype	Mutation rate[a] ($\times 10^{-8}$)	Ty1 fraction[b]	Estimated transposition rate[c] ($\times 10^{-8}$)
DG1501	*ssl2-rtt*	8.1 ± 2.3	19/24	6.4
JC297	*SSL2*	4.9 ± 1.4	3/24	0.61
DG1721	*ssl2-rtt*	13.0 ± 4	20/24	11
DG1725	*SSL2*	3.5 ± 1	3/23	0.46

[a] Rate of canavanine-resistance per cell per generation as determined by the method of Drake (1970). (±95% confidence interval.)
[b] Independent *can1* mutants were examined by PCR to determine whether a 2.3-kb region spanning the *CAN1* gene contained a Ty1 insertion.
[c] Product of mutation rate and Ty1 fraction.

plasmid YCp50 (pOY1) was introduced into DG1722 and GRF167, and Ty1-912/H3*his3-AI* transposition rates were determined in the resulting transformants, DG1721 and DG1725, respectively. The 180-fold stimulation in the rate of His^+ formation observed in DG1721 (*ssl2-rtt*) is comparable to the increase in transposition we obtained with the genomic Ty1-270*his3-AI* element in congenic *SSL2* and *ssl2-rtt* strains.

Ty1 retrotransposition and target site preferences: To characterize *ssl2-rtt*-stimulated Ty1 transposition events at specific chromosomal targets, we compared the efficiency and target site preferences of Ty1 insertions at the *CAN1* and glycine tRNA genes in *ssl2-rtt* and *SSL2* strains. These genes have been shown to be reliable targets for measuring the efficiency and insertion site preferences of Ty1 elements (Wilke *et al.* 1989; Rinckel and Garfinkel 1996; Ji *et al.* 1993; Devine and Boeke 1996). The *CAN1* gene encodes an arginine permease (Broach *et al.* 1979). Loss of gene function at this locus causes resistance to canavanine, a toxic arginine analog. Two pairs of *ssl2-rtt* and *SSL2* strains were used: the congenic strains DG1501 (*ssl2-rtt*) and JC297 (*SSL2*), and the isogenic strains DG1721 (*ssl2-rtt*) and DG1725 (*SSL2*). The spontaneous rate of mutation to canavanine resistance was 1.6- or 3.7-fold higher in the *ssl2-rtt* mutant strains DG1501 or DG1721 when compared to the rate obtained in the parental strains JC297 or DG1725, respectively (Table 3). To determine the fraction of *can1* mutants that were caused by Ty1 insertional mutagensis, 23 or 24 independent mutants from each strain were analyzed by PCR for Ty1 insertions within a 2.3-kb interval spanning the *CAN1* locus as described by Rinckel and Garfinkel (1996). The fraction of spontaneous Ty1-induced *can1* mutants increased by six-fold in the *ssl2-rtt* mutants. Therefore, the overall rate of transposition into *CAN1* increased between 10.4- to 24-fold in the *ssl2-rtt* mutant. Rate measurements at *CAN1* obtained in both sets of experiments were also used to determine whether all of the observed increase in *can1* mutations was due to Ty1 insertions. Since the average rate of non-Ty1-induced mutagenic events is about the same in *SSL2* strains (3.7×10^{-8}) as in the *ssl2-rtt* strains (2×10^{-8}), Ty1 transposition can account for the weak mutator phenotype observed at *CAN1* in the *ssl2-rtt* strains.

To address the possibility that the apparent increase in transposition rate at *CAN1* was caused by expression bias in the *ssl2-rtt* mutant (DG1721), we reintroduced the wild-type *SSL2* gene by mating all of the Ty1-induced *can1* mutants obtained from DG1721 with DG1044 (*mat-Δ::URA3 can1 SSL2*). Since *can1* and *ssl2-rtt* mutations are recessive, the diploid strains should become sensitive to canavanine if the Ty1-induced *can1* mutations were dependent on *ssl2-rtt*. Inclusion of the *mat* mutation was in DG1044 eliminated the regulatory effects of the *MAT* locus on Ty1 transcription in diploids (Errede *et al.* 1980). All of the Ty1-induced *can1* mutants remained canavanine-resistant in the *ssl2-rtt/SSL2* diploid, whereas the diploids made with the parental strains DG1721 and DG1725 were canavanine-sensitive. Therefore, expression bias does not account for the increase in Ty1-induced mutagenesis at *CAN1*.

The insertion sites of spontaneous Ty1 transposition events in DG1721 (*ssl2-rtt*) and DG1725 (*SSL2*) were obtained by sequencing the 5′ Ty1/*CAN1* junction to determine whether the *ssl2-rtt* mutation affected target site preferences. The GRF167 strain background was advantageous to use for target site analysis because we have mapped a large number of pGTy1-H3*his3-AI* insertions at *CAN1* in this strain (Rinckel and Garfinkel 1996). In DG1721, 40% (8/20) of the Ty1 insertions were distributed throughout the 300-bp *CAN1* promoter region, while the remaining 60% (12/20) were inserted in *CAN1* coding sequence. All insertions appeared normal, as suggested by the presence of a typical 5-bp target site duplication at the 5′ Ty1/*CAN1* junction. Chi square analysis ($\chi^2 = 1.2$; $P = 0.2$) suggests that the insertion sites utilized by Ty1 in the *ssl2-rtt* mutant resemble those utilized when pGTy1-H3*his3-AI* was induced in the parental *SSL2* strain GRF167 [53% promoter insertions

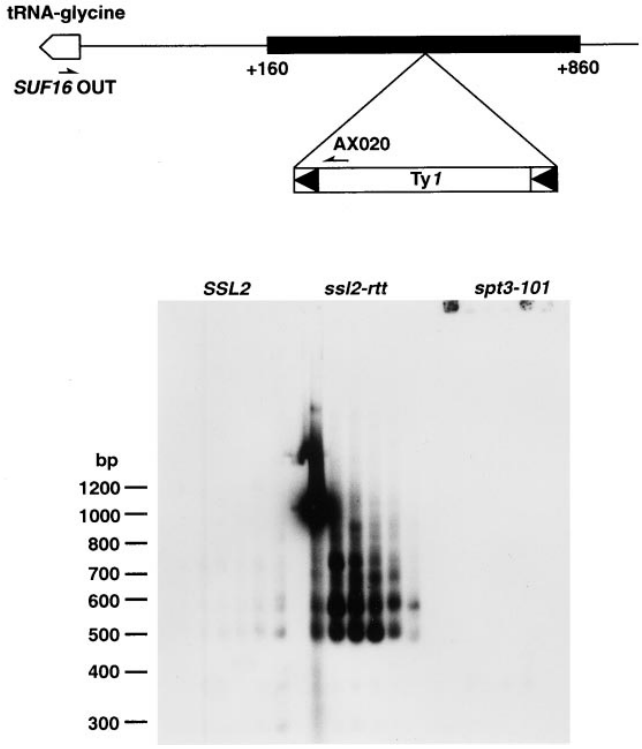

Figure 2.—*ssl2-rtt* increases the spontaneous Ty1 and Ty2 transposition events upstream of glycine tRNA genes. Schematic representation of a typical glycine tRNA gene is at the top. tRNA gene and direction of transcription is shown by the open arrow. Ty1 [for simplicity we will refer to all the transposition events detected in this assay as resulting from Ty1 elements; however, Ty2 insertions may also be present (Curcio *et al.* 1990)] insertions occur between 160 and 860 base pairs (bp) upstream of one or more of the 16 glycine tRNA genes dispersed in the yeast genome. Oligonucleotide primers used for PCR amplifications are designated *SUF16* OUT and AX020, which are homologous with glycine tRNA genes, and Ty1 and Ty2 elements, respectively. Below are the patterns of Ty1 insertions upstream of the glycine tRNA genes from the isogenic strains GRF167 (*SSL2*), DG1722 (*ssl2-rtt*), and DG789 (*spt3-101*). DNA from 6 independent colonies of each strain was analyzed by PCR using a ^{32}P-labeled *SUF16* OUT primer and an unlabeled AX020 primer. PCR products were separated by electrophoresis on a 2% agarose gel. The gel was dried and autoradiographed. Alongside the autoradiograph are size standards in base pairs (bp).

(67/126) and 47% (59/126) coding sequence insertions; Rinckel and Garfinkel 1996]. All of the Tyl promoter insertions were in the same transcriptional orientation as that of the *CAN1* gene, a bias that has been observed previously. Therefore, the *ssl2-rtt* mutation allows the normal spectrum of *CAN1* insertion sites to be used 10.4- to 24-fold more efficiently.

To determine whether the *ssl2-rtt* mutation affected Ty transposition in an unselected population of cells, we modified the genetic footprinting technique of Smith *et al.* (1995) so that spontaneous unmarked Tyl (and Ty2) insertions could be monitored at a known Ty1 hotspot (Figure 2). Genomic regions upstream of the 16 dispersed glycine tRNA genes were chosen because this region of the *SUF16* glycine tRNA gene on chromosome III is a hotspot for Ty1 transposition in transposition-induced cells (Ji *et al.* 1993; Devine and Boeke 1996). GRF167 (*SSL2*), DG1722 (*ssl2-rtt*), and DG789 (*spt3-101*) were grown on YPD plates for 7 days at 20°. Six colonies per strain were then inoculated into individual YPD liquid cultures. After two days incubation at 20°, DNA was prepared from each of the six cultures for PCR analysis. The PCR reactions for detecting Ty insertions contained a ^{32}P-labeled primer homologous to sequences within 16 glycine tRNA genes (*SUF16* OUT) and an unlabeled Ty primer (AX020) homologous with the polypurine tract of Ty1 and Ty2 elements. We will refer to all the transposition events detected in this assay as resulting from Ty1 elements; however, some Ty2 insertions may also be present (Curcio *et al.* 1990). The resulting products were separated by agarose gel electrophoresis and visualized by autoradiography. When the Ty1 insertion pattern of DG1722 (*ssl2-rtt*) is compared to GRF167 (*SSL2*) and DG789 (*spt3-101*), the *ssl2-rtt* mutation greatly stimulates the level of Ty1 transposition events upstream of glycine tRNA genes. Similar insertion patterns and product yield detected by PCR within each group of six independent cultures provide evidence that similar insertion sites were utilized. The majority of Ty1 insertions occurred between 160 and 860 bp upstream of the glycine tRNA genes in GRF167 (*SSL2*) and DG1722 (*ssl2-rtt*), and the pattern of insertions was also similar. An exceptionally intense band in one of the DG1722 cultures suggests that a Ty1 insertion occurred very early in cell growth, creating a "jackpot" event. A negative control was provided by DG789, a *spt3-101* derivative of GRF167, in which Ty1 transcription (Winston *et al.* 1984) and transposition (Boeke *et al.* 1986) is severely reduced. All DNA samples were PCR-competent, as demonstrated from control reactions in which oligonucleotide primers specific to the *TRP1* gene were substituted for primers *SUF16* OUT and AX020 (data not shown). Our results suggest that the hotspot upstream of glycine tRNA genes is utilized more efficiently by Ty1 in the *ssl2-rtt* background. Since the regions upstream of 16 dispersed glycine tRNA genes including *SUF16* are being monitored in this experiment, we cannot distinguish the relative contribution of each locus to the total transposition signal.

Level of Ty1 cDNA and chromosomal recombination: To determine if *ssl2-rtt* stimulates both Ty1 cDNA recombination and transposition or just Ty1 transposition, we performed a Ty1*his3-AI* transposition assay in a *rad52 ssl2-rtt* double mutant (Table 2C and 2D). Ty1 transposition is moderately elevated in a *rad52* mutant background (Curcio and Garfinkel 1994), but cDNA recombination is strongly dependent on *RAD52* (Sharon *et al.* 1994). The appropriate strains were made by crossing DG1501 with DG1520, a *rad52-hisG::URA3* mutant that was derived from a strain (JC364) closely related to

TABLE 4

Effect of *ssl2-rtt* on mitotic recombination

Strain	Relevant genotype	Heteroalleles	Recombination rate ($\times 10^{-6}$)
DG1751	*ssl2-rtt*	*ade2-5′Δ-TRP1-ade2-n*	50
yAR71	*SSL2*	*ade2-5′Δ-TRP1-ade2-n*	44
DG1758	*ssl2-rtt*	*MUSH21/18-trp1*	0.12
GRY1658	*SSL2*	*MUSH21/18-trp1*	0.1

Rate of Ade^+ or Trp^+ recombinants per cell per generation as determined by the method of Drake (1970).

the parental *SSL2* strains JC297 and JC358. Fifteen tetrads were analyzed and representative *rad52-hisG::URA3* (DG1636), *ssl2-rtt* (DG1637), *rad52-hisG::URA3 ssl2-rtt* (DG1638), and *RAD52 SSL2* (DG1639) ascosporal derivatives were chosen to determine Ty1-270*his3-AI* transposition rates (Table 2C and 2D). As expected, the *rad52-hisG::URA3* mutants (DG1520 and DG1636) had higher transposition rates than the *RAD52* strains (JC364 and DG1639). The transposition rate was about 40-fold higher in the *ssl2-rtt rad52-hisG::URA3* mutant (DG1638) than in the *rad52-hisG::URA3* mutant (DG1636). This result suggests that *ssl2-rtt* primarily stimulates Ty1 transposition and not cDNA recombination, because the *ssl2-rtt*-mediated increase in Ty1 transposition is independent of *RAD52*. The rate of Ty1-270*his3-AI* transposition was also about two-fold higher in the *rad52-hisG::URA3 ssl2-rtt* double mutant (DG1638) than in the *ssl2-rtt* strain (DG1637), suggesting that *RAD52* and *SSL2* belong to different epistasis groups with respect to inhibiting Ty1 transposition.

Since certain mutations in the NER/TFIIH subunit gene *RAD3* stimulate the frequency of mitotic recombination (Montelone *et al.* 1988; Song *et al.* 1990; Bailis *et al.* 1995), we determined whether *ssl2-rtt* affected the overall frequency of mitotic recombination using *ade2* or *trp1* heteroalleles present in inverted repeat orientations at the *MAT* or *HIS3* loci, respectively (Table 4). Appropriate strains were made by a genetic cross (DG1751) or two-step gene transplacement (DG1758), and mitotic recombination rates were determined as described by Rattray and Symmington (1994). The *ssl2-rtt* mutant strains DG1751 and DG1758, and *SSL2* parental strains yAR71 and GRY1658 had similar rates of mitotic recombination at either the *ade2* or *trp1* loci, respectively. Taken together, these results indicated that Ty1-270*his3-AI*-mediated His^+ formation faithfully reflects the overall level of Ty1 transposition in the cell, and that mitotic recombination remains at wild-type levels in the *ssl2-rtt* mutant strains.

Other *ssl2* alleles influence Ty1 transposition: We analyzed four *SSL2*/RAD25 alleles for their ability to modulate Ty1 transposition using the Ty1-270*his3-AI* assay. The *SSL2-1* mutation was originally isolated as a dominant suppressor of *his4-316*, a mutation created by a 36-bp insertion with perfect dyad symmetry placed in the 5′ untranslated region of *HIS4* (Cigan *et al.* 1988; Gulyas and Donahue 1992). The *ssl2-x/p* and *rad25-799am* mutations contain a 3′ truncation of the gene that should eliminate 94 and 45 C-terminal amino acid residues, respectively, from the Ssl2p/Rad25p (Gulyas and Donahue 1992; Park *et al.* 1992). These mutations were designed to resemble the truncated protein predicted to be present in a XP patient (Weeda *et al.* 1990). The final mutation analyzed, *ssl2-dead*, contains a mutation in nucleotide binding motif II (Walker *et al.* 1982) of the Ssl2p DNA helicase (Gulyas and Donahue 1992).

Strains containing these mutations, as well as *ssl2-rtt*, were constructed either by a plasmid shuffle in which a plasmid-borne copy of the wild-type *SSL2* gene was replaced with centromere plasmids containing *ssl2-rtt*, *SSL2-1*, *ssl2-x/p*, or *ssl2-dead* in a *ssl2::TRP1* disruption background, or by two-step gene transplacement in the case of the *rad25-799am* mutation. All strains had the expected phenotypes, except that DG1777 (*ssl2-x/p*) did not grow at 37°. This result is somewhat surprising since DG1653 (*rad25-799am*) also contains a C-terminal truncation of Ssl2p and is sensitive to UV radiation, but grows well at 37°. The *rad25-799am* mutation failed to complement the UV-sensitivity of the *ssl2-x/p* allele, but did complement the temperature-sensitive phenotype of *ssl2-x/p*. When the rates of Ty1 transposition were determined in these strains, only *rad25-799am* did not markedly stimulate transposition (Table 5). The *ssl2-dead* and *ssl2-rtt* mutations caused the strongest Rtt^- phenotypes, whereas *SSL2-1* and *ssl2-x/p* had slightly weaker effects. The transposition rate of the *ssl2-rtt* strain DG1775 (Table 5) was more than 10-fold lower than the rate in DG1501 and DG1502 (Table 2A), even though the *SSL2* parental strains (DG1772 and JC297) had comparable transposition rates. This difference in transposition rate probably results from a low copy gene-dosage effect of the *ssl2-rtt*/pRS416 plasmid in strain DG1775 and applies to the other *ssl2* plasmids as well.

SSL2-1 was found to be recessive with respect to stimulating Ty1 transposition by two genetic tests, even though it is a dominant suppressor of *his4-316*. In the first dominance test, no change in the Rtt phenotype was observed when a *SSL2-1/LEU2-CEN* plasmid was in-

TABLE 5

Allele-specific stimulation of Ty1 transposition

Strain	Relevant genotype	Transposition rate[a] ($\times 10^{-7}$)	Fold-increase[b] (mutant/wild-type)
DG1775	*ssl2-rtt*	19	19
DG1776	*ssl2-dead*	24	24
DG1777	*ssl2-x/p*	8	8
DG1772	*SSL2*	1	1
DG1778	*SSL2-1*	6	10
DG1774	*SSL2*	0.6	1
DG1653	*rad25-799am*	2	2
JC297	*SSL2* (*RAD25*)	1	1
BLY15	*rad3-rtta*	13	41
BLY18	*rad3-rttb*	5.4	17
BLY14	*RAD3*	0.3	1

[a] Rate of His^+ prototroph formation per cell per generation as determined by the method of Drake (1970).
[b] Mutant transposition rate over the wild-type rate for each set of strains.

troduced into the *SSL2* strain JC364, as monitored by the qualitative Ty1-270*his3-AI* transposition assay. In the second test, we utilized the plasmid shuffle technique described above to create strains containing a chromosomal *ssl2::TRP1* null mutation, and centromere plasmids with *SSL2-1* or *SSL2*. The increased level of Ty1 transposition observed with the *SSL2-1* mutant was reduced to wild-type levels when the *SSL2*/pRS416 plasmid was also present in the same cell.

The *ssl2-rtt* mutation does not suppress *his4-316*: Since *SSL2-1* was identified as an extragenic suppressor of *his4-316*, we determined whether *ssl2-rtt* also suppresses *his4-316*. Gulyas and Donahue (1992) reported that *ssl2-x/p* does not suppress *his4-316*; *ssl2-dead* was not analyzed in their study. We constructed a *ssl2-rtt* strain (DG1793) that is isogenic with the *SSL2-1* strain JJ586 and the parental *SSL2* strain JJ565 by two-step gene transplacement. As expected, *SSL2-1* suppressed the *his4-316* mutation. Cells containing *his4-316*, and *SSL2* or *ssl2-rtt* grew poorly on media lacking histidine after extended incubation of 7 days. All strains grew well when histidine was added to the medium. These results indicate that *ssl2-rtt* does not suppress *his4-316*.

Posttranslational regulation of Ty1 transposition by *SSL2*: To determine whether the *ssl2-rtt* mutation affects Ty1 or Ty1*his3-AI* RNA levels, quantitative Northern hybridizations were performed with RNA extracted from cells grown under the same conditions as those used for measuring Ty1*his3-AI* transposition (Figures 3 and 4). Most of the analyses were performed with RNA extracted from mid-to-late log phase cells. An additional experiment was included using RNA extracted from stationary-phase cells to examine the effects of another growth phase on Ty1 and Ty1-*his3-AI* RNA levels (Figure 4, lanes 7–8). In the first set of experiments (Figure 3), phosphorimage analysis of the hybridization filters showed no increase in the steady-state level of total Ty1 or Ty1-270*his3-AI* RNA relative to control transcripts from genes transcribed by RNA Pol II (*ACT1* and *LYS2*) or Pol I (18S rRNA) when the *ssl2-rtt* strains DG1501 and DG1502, and the congenic parental strains JC297 and JC358 were compared.

Since the loading controls in the preceding experiment were transcripts from genes either transcribed by RNA Pol I or Pol II, there may be unforeseen effects on transcription of these genes in a *ssl2-rtt* mutant. Qiu *et al.* (1993) reported that *rad25-ts24* affects both RNA Pol II transcription and rRNA synthesis at the nonpermissive temperature, but it does not affect the rate of RNA Pol III-mediated transcription of isoleucine tRNA genes, as monitored using a hybridization probe homologous with the rapidly-processed isoleucine tRNA intron. Therefore, we examined additional *ssl2* mutants using an isoleucine tRNA ($tRNA^I$) as a loading control in a second set of Northerns that were quantitated by phosphorimage analysis (Figure 4). Total RNA was prepared from the isogenic strains DG1725 (*SSL2*; lane 1) and DG1721 (*ssl2-rtt*; lane 2), and isogenic strains DG1774 (*SSL2*; lane 3), DG1775 (*ssl2-rtt*; lane 4), DG1776 (*ssl2-dead*; lane 5), and DG1778 (*SSL2-1*; lane 6) and treated as described above, except that strains DG1721 and DG1725 were grown in SC-Ura medium to select for plasmid pOY1. The results show that total Ty1 (lanes 1–6), Ty1-912/H3*his3-AI* (lanes 1 and 2), and Ty1-270*his3-AI* (lanes 3–6) RNA levels were not altered by the *ssl2* mutations when normalized to the isoleucine pre-tRNA level. Ty1 RNA levels also remained unaltered when DG1774 (*SSL2*; lane 7) and DG1775 (*ssl2-rtt*; lane 8) were grown to stationary phase.

The formation of the mature Ty1 proteins is indicative of high levels of transposition, and therefore, may be one of the steps in the retrotransposition cycle subject to inhibition (Curcio and Garfinkel 1992). To examine the expression of Ty1 proteins, we initially determined the level of β-galactosidase activity from a genomic Ty1::*lacZ* gene fusion in which the *E. coli lacZ* gene

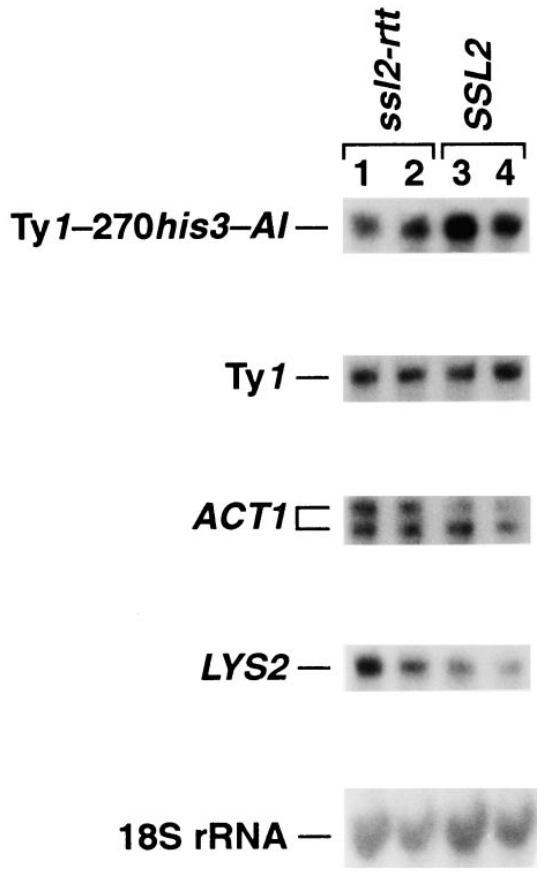

Figure 3.—Level of Ty1-270*his3-AI* and Ty1 RNA is unchanged in the *ssl2-rtt* mutant. Northern analysis of congenic *ssl2-rtt* strains DG1501 (lane 1) and DG1502 (lane 2), and *SSL2* parental strains JC297 (lane 3) and JC358 (lane 4). Cells were grown to mid-to-late log phase in YPD broth at 20°. Ten micrograms of total RNA extracted from each cell culture was separated by electrophoresis on a 1% agarose gel, and blotted to Hybond N membranes. In the top two panels, filters were hybridized with radiolabeled probes specific for *his3-AI* and Ty1. In the next three panels, filters were hybridized with probes specific for *ACT1* (actin) and *LYS2* transcripts, and 18S rRNA to ensure that equivalent amounts of RNA were analyzed from these strains.

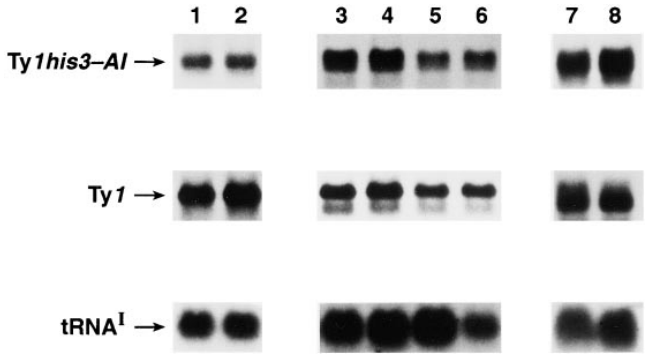

Figure 4.—Levels of Ty1-912/H3*his3-AI*, Ty1-270*his3-AI*, and Ty1 RNA remain unaltered in various *ssl2* mutants. Northern analysis of isogenic strains DG1725 (*SSL2*; lane 1) and DG1721 (*ssl2-rtt*; lane 2), and isogenic strains DG1774 (*SSL2*; lane 3), DG1775 (*ssl2-rtt*; lane 4), DG1776 (*ssl2-dead*; lane 5), and DG1778 (*SSL2-1*; lane 6) was performed as described in Figure 3 except that DG1721 and DG1725 were grown in SC-Ura medium to select for the maintenance of pOY1. Northern analysis of strains DG1774 (*SSL2*; lane 7) and DG1775 (*ssl2-rtt*; lane 8) grown to stationary phase was also included to examine Ty1 RNA levels under another growth condition. In the top panel, a ^{32}P-labeled *his3-AI* DNA probe was used to detect Ty1-912/H3*his3-AI* (lanes 1 and 2) or Ty1-270*his3-AI* (lanes 3–8) RNA levels. In the middle and lower panels, DNA probes specific for Ty1 and the isoleucine tRNA intron (tRNA^{I}) were used to detect Ty1 RNA and isoleucine pre-tRNA levels, respectively.

was inserted in-frame in the IN coding region of a chromosomal Ty1 element. β-galactosidase assays were performed on total cell extracts from *ssl2-rtt* and wild-type strains. There was no apparent difference in β-galactosidase activity between the *SSL2* strains JC297 (4.4 units) and JC358 (2.5 units), and the *ssl2-rtt* mutants DG1501 (4.5 units) and DG1502 (2.7 units). S288C and GRF167, which lack the Ty1::*lacZ* fusion, had 0.5 units and 0.4 units of activity, respectively. We also determined that the *ssl2-rtt* mutation did not change the level of *TYA1-TYB1* frameshifting (data not shown), as monitored by expression of *lacZ* fusions with or without the Ty1 frameshift signal (Belcourt and Farabaugh 1990).

To determine whether the *ssl2* mutations affected the level of endogenous Ty1 proteins, total cell protein (Figure 5) or partially purified Ty1-VLPs (Figure 6) were analyzed by immunoblotting using antisera that recognize TyA1 protein p54 and its full-length precursor p58, IN, or RT/RH. The level of TyA1 proteins was analyzed from mid-to-late log phase cells (Figure 5, lanes 2–8) and from stationary phase cells (Figure 5, lanes 9 and 10). The immunoblots included proteins from the *SSL2* strain DG1741 (pGTy1-H3*his3-AI*) that had been induced for transposition by growth in galactose to mark the positions of Ty1 proteins. Protein was also analyzed from the *spt3-101* mutant DG789 that is defective for Ty1 expression. An immunoblot from a SDS-polyacrylamide gel loaded with equal amounts of total cell protein (Figure 5) from isogenic strains DG1741 (pGTy1-H3*his3-AI*; lane 1), DG789 (*spt3-101*; lane 2), DG1722 (*ssl2-rtt*; lane 3), GRF167 (*SSL2*; lane 4), and isogenic strains DG1774 (*SSL2*; lane 5), DG1775 (*ssl2-rtt*; lane 6), DG1776 (*ssl2-dead*; lane 7), and DG1778 (*SSL2-1*; lane 8) was incubated with VLP (Figure 5A) or Hts1 antisera (Figure 5B) to detect TyA1 proteins or heat shock protein Hts1p, respectively. The amount of endogenous p58-TyA1 and p54-TyA1 was about the same for all of the strains when normalized to the total protein present or the Hts1p loading control by Ponceau S staining and laser densitometry. Similar TyA1 protein levels were observed when total protein was extracted from DG1774 (*SSL2*; lane 9) and DG1775 (*ssl2-rtt*; lane 10) strains that had been grown to stationary phase. In agreement with the immunoblot analysis, pulse-chase immunoprecipitations of TyA1 proteins suggest that the kinetics of pro-

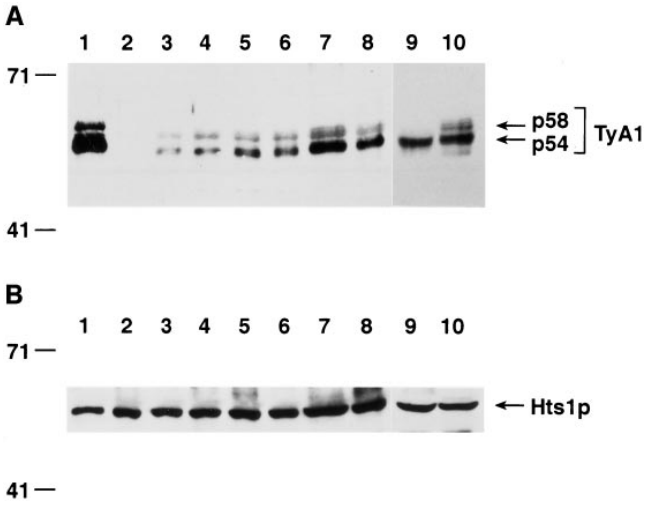

Figure 5.—Levels of endogenous TyA1 proteins are not altered in various *ssl2* mutants. Total cell protein extracts were prepared from isogenic strains DG1741 (*SSL2*, pGTy1-H3*his3-AI*; lane 1), DG789 (*spt3-101*; lane 2), DG1722 (*ssl2-rtt*; lane 3), and GRF167 (*SSL2*; lane 4), and isogenic strains DG1774 (*SSL2*; lane 5), DG1775 (*ssl2-rtt*; lane 6), DG1776 (*ssl2-dead*; lane 7), and DG1778 (*SSL2-1*; lane 8) that had been grown in either SC-Ura galactose (lane 1) or YPD (lanes 2–8) to mid-to-late log phase. Total cell protein from strains DG1774 (*SSL2*; lane 9) and DG1775 (*ssl2-rtt*; lane 10) grown to stationary phase was also included to examine TyA1 protein level under another growth condition. Transposition-induced strain DG1741 (lane 1; approximately 0.5 μg) served as a marker for endogenous TyA1 proteins from the other strains (lanes 2–10). Approximately 15 μg of total protein was loaded in lanes 2–10, separated by 7.5% SDS-polyacrylamide gel electrophoresis (SDS-PAGE), transferred to an Immobilon P membrane, and incubated with VLP (A) or Hst1p(B) polyclonal antisera. Immunodetection was performed using enhanced chemiluminescence (ECL) (Amersham). The position of molecular size markers in kilodaltons (kD), TyA1 proteins p58 and p54, and Hts1p are shown alongside the figure.

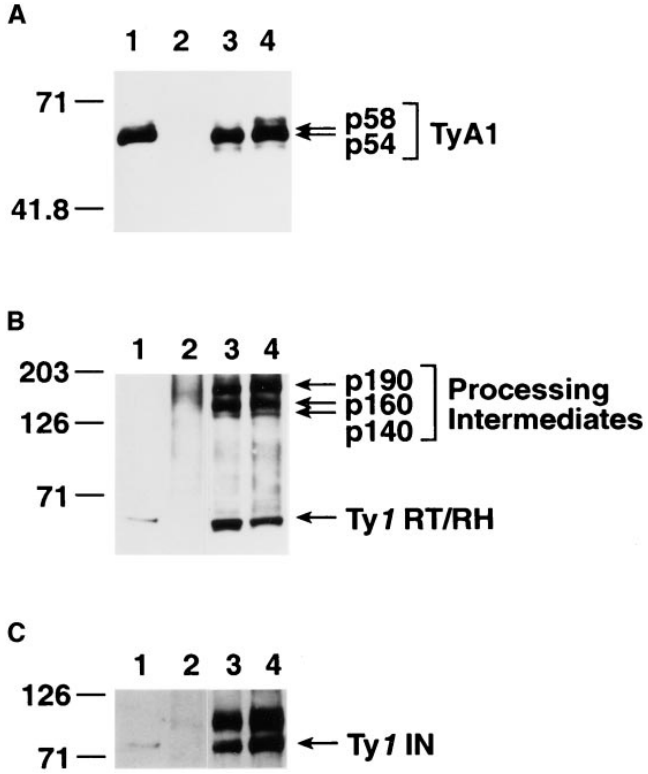

Figure 6.—Levels of TyA1 and TyB1 proteins from endogenous VLPs isolated from *SSL2* wild-type and *ssl2-rtt* mutant strains are unaltered. Partially purified VLPs were isolated from isogenic strains DG1741 (*SSL2*, pGTy1-H3*his3-AI*; lane 1), DG789 (*spt3-101*; lane 2), GRF167 (*SSL2*; lane 3), and DG1722 (*ssl2-rtt*; lane 4) and separated by 8% SDS-PAGE. (A) Approximately 0.3 μg of protein was analyzed in lanes 2–4, (B and C) 15 μg of protein was analyzed in lanes 2–4, and (A) 0.02 μg and (B and C) 0.3 μg of protein was added in lane 1. The amount of protein was adjusted because of the greater abundance of TyA1 proteins compared to TyB1 proteins in the cell, and because DG1741 was induced for transposition prior to VLP isolation. VLPs from DG1741 (lane 1) served as a marker for Ty1 proteins. After transfer to Immobilon P membranes, individual blots were incubated with either (A) VLP, (B) RT/RH, or (C) IN polyclonal antisera. Immunodetection was performed using ECL. Molecular size standards (kD) and positions of proteins are indicated.

tein processing remain unaltered in a *ssl2-rtt* mutant (data not shown).

To determine whether *ssl2-rtt* affects the level of mature Ty1 IN and RT/RH, we partially purified endogenous Ty1-VLPs by sucrose-step gradient centrifugation and analyzed equivalent samples of Ty1 proteins by immunoblotting (Figure 6). This approach was necessary because we could not detect mature IN or RT/RH in total cell extracts from *ssl2-rtt* or *SSL2* strains DG1722 and GRF167, respectively (data not shown). VLPs were isolated from DG1741 (*SSL2*; pGTy1-H3*his3-AI*; lane 1), DG789 (*spt3-101*; lane 2), GRF167 (*SSL2*; lane 3), and DG1722 (*ssl2-rtt*; lane 4) and the resulting filters were incubated with antisera against VLPs (Figure 6A), RT/RH (Figure 6B), and IN (Figure 6C). p54 was the major TyA1 protein present in VLPs from transposition-induced cells (Figure 6A, lane 1), and in endogenous VLPs from *SSL2* (Figure 6A, lane 3) and *ssl2-rtt* (Figure 6A, lane 4) strains. The RT/RH antiserum (Figure 6B) reacted with the p190 (TyA1-TyB1), p160 (PR-IN-RT/RH), and p140 (IN-RT/RH) precursors and mature RT/RH (p60) present in endogenous VLPs from the *SSL2* (Figure 6B, lane 3) and *ssl2-rrt* (Figure 6B, lane 4) strains. Similar results were obtained when IN antiserum was used (Figure 6C, lanes 3 and 4; data not shown). Mature p54-TyA1, RT/RH, and IN obtained from endogenous *SSL2* (lane 3) and *ssl2-rtt* (lane 4) VLPs had similar electrophoretic mobilities as the cognate proteins from transposition induced cells (lane 1). Similar amounts of Ty1 proteins were present in the VLPs from *SSL2* and *ssl2-rtt* strains. As expected, Ty1 proteins were not detected from DG789 (lane 2).

These results suggest that *SSL2* inhibits Ty1 transposition at the posttranslational level. If Ty1 VLP functions are inhibited by *SSL2*, then VLPs isolated from a *ssl2-*

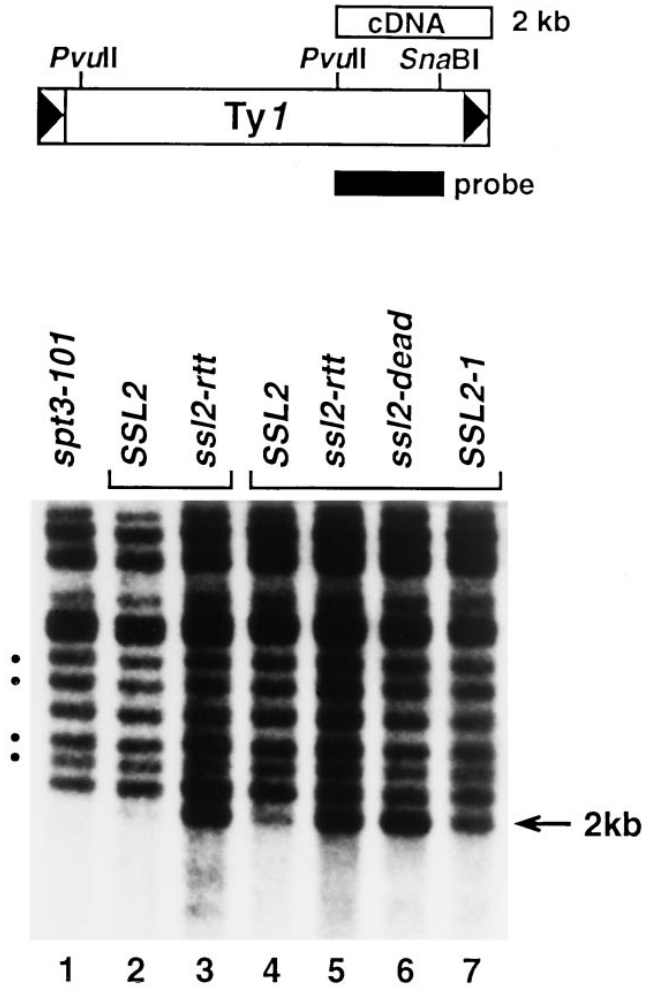

Figure 7.—Ty1 cDNA is increased in *ssl2* mutants. The 2-kb segment of Ty1 cDNA detected by Southern analysis of total yeast DNA digested with *Pvu*II is shown on the top. A Ty1 element is depicted along with relevant *Pvu*II (nucleotide positions 475 and 3944) and *Sna*BI (position 5461) restriction sites (Boeke *et al.* 1988). Additional Ty1 element features are described in Figure 1. Solid bar represents the *Pvu*II-*Sna*BI restriction fragment used as Southern hybridization probe to detect Ty1 cDNA. Total DNA was isolated after strains DG789 (*spt3-101*; lane 1), GRF167 (*SSL2*; lane 2), DG1722 (*ssl2-rtt*; lane 3), DG1774 (*SSL2*; lane 4), DG1775 (*ssl2-rtt*; lane 5), DG1776 (*ssl2-dead*; lane 6), and DG1778 (*SSL2-1*; lane 7) were grown to mid-to-late log phase, digested with *Pvu*II, and subjected to Southern analysis using a ^{32}P-labeled probe spanning the Ty1 RT/RH region (nucleotides 3944–5461). Positions of the 2-kb Ty1 cDNA and four conserved Ty1-chromosomal junction fragments (●) used for normalization are shown alongside the figure.

rtt strain may have an increased level of reverse transcriptase or integrase activities *in vitro*. However, we were not able to reproducibly detect these activities from endogenous VLP preparations from either *SSL2* or *ssl2-rtt* strains, because of their low abundance and the presence of cellular inhibitors (data not shown). As expected, the level of pGTy1-H3*his3-AI* and VLP production is greatly stimulated in a transposition-induced *SSL2* wild-type strain. However, *ssl2-rtt* does not markedly affect transposition or VLP production under transposition-inducing conditions when compared to wild-type *SSL2*. Since we showed that galactose induction of pGTy1 overcomes posttranslational control of Ty1 transposition (Curcio and Garfinkel 1992), pGTy1 expression in *SSL2* cells may override the negative effects of Ssl2p.

Ty1 cDNA is increased in *ssl2* mutants: Since we had difficulty identifying relevant biochemical activities from endogenous Ty1 VLPs, we determined whether the level of linear Ty1 cDNA increased in *ssl2* mutants (Figure 7). Total DNA was prepared after the strains were grown to mid-to-late log phase at 20°, digested with *Pvu*II, and subjected to Southern blot hybridization using a ^{32}P-labeled probe spanning the RT/RH region at the 3′ end of Ty1. The probe should detect an unintegrated Ty1 cDNA fragment of about 2 kb that contains sequences from the *Pvu*II site at nucleotide 3944 to the end of the element at nucleotide 5918 [coordinates are taken from the sequence of Ty1-H3 (Boeke *et al.* 1988)]. The probe should also hybridize with integrated Ty1 elements present in the genome, generating a variety of different fragments that contain Ty1 sequences joined to genomic DNA.

When the level of Ty1 cDNA (Figure 7) present in total cellular DNA from isogenic strains GRF167 (*SSL2*; lane 2) and DG1722 (*ssl2-rtt*; lane 3) was estimated relative to four conserved Ty1-genomic DNA junction fragments, there was a 50-fold increase in Ty1 cDNA in the *ssl2-rtt* mutant. This analysis was extended to additional *ssl2* mutants in which Ty1 transposition was increased (Table 5). We observed that the cDNA level was elevated 7-fold in DG1775 (*ssl2-rtt*; lane 5), 12-fold in DG1776 (*ssl2-dead*; lane 6), and 5-fold in DG1778 (*SSL2-1*; lane 7) when compared to strain DG1774 (*SSL2*; lane 4). As noted previously with the transposition rates (Tables 2A and 5), the increase in the level of Ty1 cDNA with a plasmid-borne *ssl2-rtt* mutant DG1775 was less than that obtained with a chromosomal *ssl2-rtt* mutant. This difference in cDNA level probably results from a low copy gene-dosage effect of the *ssl2-rtt*/pRS416 plasmid and applies to the other *ssl2* plasmids as well. As expected, we could not detect Ty1 cDNA in the *spt3-101* strain DG789 (lane 1), even after extended autoradiography. The level of Ty1 cDNA also increased when partially purified endogenous VLPs from DG1722 were examined (data not shown).

***rtt* alleles of *RAD3*:** To determine whether other NER/TFIIH subunits inhibit Ty1 transposition, we analyzed a highly UV-sensitive *RAD3* allele, *rad3-2* (Montelone *et al.* 1988), and also searched for new *RAD3* mutations that stimulate Ty1 transposition. A *rad3-2* mutant, RM145-3D, was backcrossed three times with *RAD3* Ty1-270*his3-AI* strains JC358 or JC364. Several *rad3-2* Ty1-270*his3-AI* derivatives from these crosses displayed normal levels of Ty1 transposition. However, two *rad3-rtt*

alleles were isolated by hydroxylamine mutagenesis (Table 5). A *TRP1* centromere plasmid containing *RAD3* (*RAD3*/pRS414) was mutagenized by treatment with hydroxylamine *in vitro*, and the plasmid was introduced into the *rad3::LEU2* strain containing a *RAD3*/*URA3*-centromere plasmid, pBM6. After nonselective growth, cells that had lost the *URA3* plasmid were selected on 5-FOA medium, and the Trp^+ Ura^- cells were analyzed for Ty1 transposition, UV-sensitivity, and growth at 37°. The *rad3-rtta* and *rad3-rttb* mutations increase the rate of Ty1-270*his3-AI* transposition by 41- and 17-fold, respectively, when compared to the isogenic *RAD3* strain. The sensitivity to UV radiation and growth phenotype at 37° was similar in the *RAD3* and *rad3-rtt* strains. Ty1 transcript and TyA1 protein levels also remained unchanged in the *rad3-rtt* mutants (data not shown).

DISCUSSION

Inhibition of Ty1 transposition by *SSL2* and *RAD3*: The association between NER/TFIIH subunits and inhibition of Ty1 transposition was discovered in two ways. *SSL2* was identified in a genome-wide mutational screen for genes that inhibit or negatively regulate Ty1 transposition. We then reasoned that if NER/TFIIH gene products inhibit Ty1 transposition, *rtt* mutations should be recovered in other genes involved in NER and TFIIH-mediated transcription. The isolation of *rad3-rtt* alleles with many of the same properties as *ssl2-rtt* and the demonstration that the *rad3* Rtt^- phenotype is also allele-specific implicate NER/TFIIH in the regulation of Ty1 transposition. Further support for NER/TFIIH inhibiting Ty1 transposition will be obtained by isolating *rtt* mutations in additional subunit genes.

To understand how *ssl2* and *rad3* mutations stimulate Ty1 retrotransposition, we examined transposition events and homologous recombination levels at various target loci, studied the allele specificity of several mutations, and determined whether the level of Ty1 gene products increases in the mutants. Our results show that *ssl2-rtt* causes an increase in Ty1 transposition, but does not influence target site selectivity, or the level of cDNA or mitotic recombination. The results of extensive Northern and immunoblot analyses indicate that the level of Ty1 and Ty1*his3-AI* transcripts, and TyA1, IN, and RT/RH proteins remain the same in various *ssl2* and *rad3* mutants. Interestingly, the level of Ty1 cDNA and rate of Ty1 transposition increase concomitantly in the *ssl2* mutants. These results suggest that NER/TFIIH subunits inhibit Ty1 retrotransposition posttranslationally by minimizing the accumulation of Ty1 cDNA.

Inhibition of Ty1 transposition and the multiple functions of NER/TFIIH: We have analyzed *SSL2* and *RAD3* mutants for phenotypes associated with TFIIH and NER. These fall into three categories: suppression of *his4-316*, sensitivity to UV radiation, and slow or temperature-sensitive growth. Suppression of *his4-316* illustrates the complexity of *SSL* genes and NER/TFIIH. Certain mutations in *SSL1* and *SSL2* suppress a stable stem-loop structure present in the leader sequence of *his4-316* (Gulyas and Donahue 1992; Wang *et al.* 1995) that prevents translation initiation (Cigan *et al.* 1988). These results initially led to the idea that Ssl1p and Ssl2p promote the secondary structure "unwinding" necessary to promote ribosomal binding/scanning of mRNA. We have analyzed *ssl2-rtt* and *SSL2-1* mutations for their effects on Ty1 transposition and *his4-316* suppression. Both of these mutations cause higher levels of Ty1 transposition, but only *SSL2-1* suppresses *his4-316* (Gulyas and Donahue 1992). Furthermore, we show that *SSL2-1* is recessive with respect to increasing Ty1 transposition, although *SSL2-1* is dominant with respect to suppressing *his4-316*. These results suggest that *SSL2-1* gains a function required for suppressing *his4-316*, loses a function required to inhibit Ty1 transposition, and that these functions may be different.

Even though *SSL2* is implicated in translation initiation and transcription, our results show that *ssl2-rtt*, *ssl2-dead*, and *SSL2-1* mutations do not increase the level of Ty1 RNA when normalized to any one of several internal standards present in total RNA from growing cultures. The *ssl2-rtt* mutation does not affect the frequency of programmed translational frameshifting required to synthesize TyB1 (Farabaugh 1995). The *ssl2-rtt*, *ssl2-dead*, and *SSL2-1* mutations do not increase the level of TyA1 in growing cultures, and *ssl2-rtt* does not affect the level of TyA1, IN and RT/RH proteins in partially purified endogenous Ty1 VLPs. Furthermore, *ssl2-rtt* does not increase Ty1 RNA and TyA1 protein levels in cells grown to stationary phase. These results suggest that *SSL2* inhibits Ty1 transposition posttranslationally.

Several results suggest that inhibition of Ty1 transposition is independent of Ssl2p and Rad3p NER functions. First, an increase in Ty1 transposition accounts for the modest mutator phenotype observed at *CAN1* in the *ssl2-rtt* mutant, suggesting that overall NER of spontaneous DNA damage is unaffected by *ssl2-rtt*. Second, *rad3* and *ssl2* mutations that cause UV-sensitivity do not markedly increase the level of Ty1 transposition. Third, with the exception of *ssl2-x/p* and *rad25-799am*, the five *rad3* and *ssl2* alleles that stimulate Ty1 transposition (*rad3-rtta*, *rad3-rttb*, *ssl2-rtt*, *ssl2-dead*, and *SSL2-1*) do not cause extreme UV-sensitivity. Both *ssl2-x/p* and *rad25-799am* mutations cause UV-sensitivity because of a defect in NER, but only the *rad25-799am* mutation fails to stimulate Ty1 transposition or affect growth. Since the *ssl2-x/p* mutation stimulates Ty1 transposition, causes temperature-sensitive growth and UV-sensitivity, this mutation probably alters other functions of Ssl2p in addition to NER. Fourth, none of the missense mutations in *SSL2* that stimulate Ty1 transposition are located in the C-terminal domain required for NER and transcription-coupled repair (Sweder and Hanawalt 1994). Fifth, *ssl2-rtt* contains the same mutation that causes the tem-

perature-sensitive phenotype of *rad25-ts24*, a conditionally lethal mutation used to show that Ssl2p (Rad25p) is required for RNA Pol II transcription (Qiu *et al.* 1993; Guzder *et al.* 1994b). Finally, null mutations in the NER genes *RAD1* and *RAD2* do not stimulate Ty1 transposition (A. J. Rattray, M. J. Curcio and D. J. Garfinkel, unpublished results).

NER/TFIIH subunits inhibit Ty1 transposition by preventing cDNA accumulation: The likelihood that the increase in Ty1 cDNA level explains the increase in Ty1 transposition in the *ssl2* mutants rests on two features of the transposition process. First, a relatively low level of cDNA competent for integration *in vitro* is associated with Ty1 VLPs purified from transposition induced cells (Eichinger and Boeke 1988, 1990). Addition of exogenous linear DNA with the proper terminal nucleotides to VLPs, however, increases integration activity up to 100-fold (Eichinger and Boeke 1990). These results suggest that completely replicated Ty1 cDNA is limiting for integration *in vitro*. Second, we observed that the level of Ty1 cDNA and Ty1*his3-AI* transposition increases to comparable degrees in various *ssl2* mutants when compared with isogenic *SSL2* parental strains. These results suggest that the level of full-length Ty1 cDNA may also limit for transposition *in vivo*, and that increasing the level of cDNA may completely account for the elevated transposition rate in the *ssl2* mutants.

We propose two models suggesting how NER/TFIIH subunits inhibit the accumulation of Ty1 cDNA. The first model suggests that NER/TFIIH subunits inhibit reverse transcription by inactivating Ty1 RT/RH or altering a replication intermediate. This inhibition is weakened in the *ssl2* and *rad3* mutants, perhaps by lowering Ssl2p or Rad3p helicase activity (see below). A complete analysis of Ty1 RT/RH activity and reverse transcription in *SSL2* and *ssl2-rtt* strains is required to address this model. Although cellular factors responsible for modulating Ty1 reverse transcription and integration are poorly understood, host proteins have been identified that stimulate murine leukemia virus (MLV) and human immunodeficiency virus integration (Kalpana *et al.* 1994; Farnet and Bushman 1997; Miller *et al.* 1997), or minimize MLV autointegration (Lee and Craigie 1994). Several chromosomal genes have also evolved to inhibit retrovirus replication. In particular, the murine *Fv1* gene blocks MLV infection after entry into the cell but before integration (Pryciak and Varmus 1992). This step in replication is shared by retroviruses and retrotransposons. However, unlike the cellular inhibitors of Ty1 transposition described here, the *Fv1* locus appears to encode a gag-like protein from an endogenous retrovirus unrelated to MLV (Best *et al.* 1996).

The second model posits that Ty1 cDNA is degraded by a nuclease complex containing Ssl2p and Rad3p helicases. The alteration in Ss12p or Rad3p activity that leads to an increase in Ty1 transposition remains to be determined. Because the *SSL2-1* mutation is located between helicase sequence motifs I and II, *ssl2-dead* maps in motif II, and *ssl2-rtt* is located between motifs III and IV (Walker *et al.* 1982), however, a change in DNA helicase activity or nucleotide binding might be responsible for increasing Ty1 transposition. The crystal structure of a related DExx box DNA helicase from *Bacillus stearothermophilus* suggests that all six of the conserved helicase motifs are involved in ATP-binding or coupling hydrolysis to helicase activity (Subramanya *et al.* 1996).

Bailis *et al.* (1995) have identified an interesting *RAD3* mutant, *rad3-G595R*, that has certain phenotypes in common with the *ssl2-rtt* mutant described here. Like *ssl2-rtt*, cells containing *rad3-G595R* are temperature sensitive and weakly UV sensitive. The *rad3-G595R* mutation specifically relaxes the restriction against homologous recombination between short ($\leq$250–300 bp) identical or mismatched DNA sequences. Although we have not examined short sequence recombination in a *ssl2-rrt* mutant, recombination involving longer regions of homology is unaltered in *ssl2-rtt* or *rad3-G595R* mutants. However, our results suggest that *ssl2-rtt* does not increase the frequency of Ty1 cDNA recombination (Sharon *et al.* 1994), which could involve short sequences with limited homology. Therefore, *ssl2-rtt* may not affect short sequence recombination. Highly UV sensitive alleles of *RAD3*, *rad3-20* or *rad3-2*, also do not alter recombination (Bailis and Maines 1996) or Ty1 transposition. Most importantly, the physical stability of chromosomal double strand breaks increases in the *rad3-G595R* mutant (Bailis *et al.* 1995; Bailis and Maines 1996), which is strikingly similar to the increased level of Ty1 cDNA observed in the *ssl2* mutants. In addition, we have characterized *rad3* alleles that increase Ty1 transposition. It should be very informative to determine whether *ssl2-rtt*, *rad3-rtta*, *rad3-rttb*, and *rad3-G595R* affect the same processes.

Neither of our models rules out the possibility that inhibition of Ty1 by NER/TFIIH subunits occurs indirectly. Another cellular protein might inhibit Ty1 transposition and also interact with NER/TFIIH subunits, but fail to interact with Rtt$^-$ NER/TFIIH subunits. A mammalian homolog of the yeast 26S proteasome component Sug1p has been identified that strongly interacts with XPB and TFIIH, but does not interact with a mutant XPB protein from a XPB patient (Weeda *et al.* 1997). Alternatively, another gene product whose transcription is very sensitive to TFIIH may inhibit Ty1 transposition posttranslationally. A similar hypothesis has been presented to explain several unusual anomalies associated with Cockayne syndrome and trichothiodystrophy, both of which can result from mutations in human *XPB* (for a review, see Lehmann 1995). A variety of phenotypes evidently unrelated to NER have also been observed in certain Drosophila *haywire* mutants (Mounkes *et al.* 1992).

Multiple pathways contribute to inhibiting Ty1 transposition: A small but growing number of genes in addition to *SSL2* and *RAD3* inhibit Ty1 transposition at the

posttranscriptional level. *RAD6* influences both the level of Ty1 transposition and target site preference at genes transcribed by RNA Pol II (Liebman and Newnam 1993). *RAD6*, through its ubiquitin conjugating activity, participates in DNA repair caused by a variety of agents such as UV and gamma radiation, and alkylating the cross-linking agents (for a review, see Lawrence 1994). *FUS3* may regulate global levels of Ty1 transposition by destabilizing Ty1 proteins (Conte *et al.* 1998). *FUS3* is a mitogen-activated protein kinase involved in pheromone signaling and a negative regulator of the haploid cell invasive growth pathway, which may be triggered by nutrient limitation (Roberts and Fink 1994). We have also identified genes involved in double strand break repair and recombination, such as *RAD52* and *RAD57*, that inhibit Ty1 transposition (A. J. Rattray, M. J. Curcio and D. J. Garfinkel, unpublished results). In addition, Ty1 RNA levels, and hence, transposition, increase when cells are exposed to UV radiation or DNA alkylating agents (Rolfe *et al.* 1986; Bradshaw and McEntee 1989). The functions of these genes suggest that pathways responsible for minimizing the effects of genomic or nutritional stress also minimize Ty1 transposition. Similar relationships between transposition and cellular stress have been observed with transposable elements in plants (for reviews, see McClintock 1984; Wessler 1996). Our studies suggest that NER/TFIIH subunits inhibit Ty1 transposition by a pathway that is different from those strictly responding to DNA damage. However, the pathways controlling these posttranscriptional and transcriptional responses of Ty1 elements have not been fully defined. Further genetic and biochemical studies of *RTT* genes should elucidate the mechanisms used by the cell to inhibit Ty1 element transposition and maintain genome stability.

We thank A. Rattray for helpful discussions, T. Mason for Hts1 antiserum, T. Donahue, T. Dunn, G. Fink, A. Hinnebusch, R. Jazwinski, B. Montelone, L. Prakash and R. Sikorski for plasmids, and T. Donahue, G. Fink, R. Malone, A. Rattray and J. Strathern for strains. Research is sponsored by the National Cancer Institute, Department of Health and Human Services, under contract with Advanced BioScience Laboratories. The contents of this publication do not necessarily reflect the views or policies of the Department of Health and Human Services, nor does mention of trade names, commercial products, or organizations imply endorsement by the United States Government. M.J.C. is funded by National Institutes of Health grant GM52072.

LITERATURE CITED

Aguilera, A., 1994 Formamide sensitivity: a novel conditional phenotype in yeast. Genetics **136:** 87–91.

Alani, E., L. Cao and N. Kleckner, 1987 A method for gene disruption that allows repeated use of *URA3* selection in the construction of multiply disrupted yeast strains. Genetics **116:** 541–545.

Atkin, A. L., N. Altamura, P. Leeds and M. R. Culbertson, 1995 The majority of yeast *UPF1* colocalizes with polyribosomes in the cytoplasm. Mol. Biol. Cell **6:** 611–625.

Bailis, A. M., and S. Maines, 1996 Nucleotide excision repair gene function in short-sequence recombination. J. Bacteriol. **178:** 2136–2140.

Bailis, A. M., S. Maines and M. T. Negritto, 1995 The essential helicase gene *RAD3* suppresses short-sequence recombination in *Saccharomyces cerevisiae*. Mol. Cell. Biol. **15:** 3998–4008.

Belcourt, M. F., and P. J. Farabaugh, 1990 Ribosomal frameshifting in the yeast retrotransposon Ty: tRNAs induce slippage on a 7 nucleotide minimal site. Cell **62:** 339–352.

Best, S., P. Le Tissier, G. Towers and J. P. Stoye, 1996 Positional cloning of the mouse retrovirus restriction gene *Fv1*. Nature **382:** 826–829.

Boeke, J. D., 1988 Retrotransposons, pp. 59–103 in *RNA Genetics, Retroviruses, Viroids, and RNA Recombination*, edited by E. Domingo, J. Holland and P. Ahlquist. CRC Press, Boca Raton, FL.

Boeke, J. D., and S. B. Sandmeyer, 1991 Yeast transposable elements, pp. 193–261 in *The Molecular and Cellular Biology of the Yeast Saccharomyces: Genome Dynamics, Protein Synthesis, and Energetics*, edited by J. R. Pringle, E. W. Jones and J. R. Broach. Cold Spring Harbor Laboratory Press, Cold Spring Harbor, NY.

Boeke, J. D., F. LaCroute and G. R. Fink, 1984 A positive selection for mutants lacking orotidine-5′-phosphate decarboxylase activity in yeast: 5-fluoroorotic acid resistance. Mol. Gen. Genet. **197:** 345–346.

Boeke, J. D., D. J. Garfinkel, C. A. Styles and G. R. Fink, 1985 Ty elements transpose through an RNA intermediate. Cell **40:** 491–500.

Boeke, J. D., C. A. Styles and G. R. Fink, 1986 *Saccharomyces cerevisiae SPT3* gene is required for transposition and transpositional recombination of chromosomal Ty elements. Mol. Cell. Biol. **6:** 3575–3581.

Boeke, J. D., D. Eichinger, D. Castrillon and G. R. Fink, 1988 The *Saccharomyces cerevisiae* genome contains functional and nonfunctional copies of transposon Ty1. Mol. Cell. Biol. **8:** 1432–1442.

Bradshaw, V. A., and K. McEntee, 1989 DNA damage activates transcription and transposition of yeast Ty retrotransposons. Mol. Gen. Genet. **218:** 465–474.

Broach, J. R., J. N. Strathern and J. B. Hicks, 1979 Transformation in yeast: development of a hybrid cloning vector and isolation of the *CAN1* gene. Gene **8:** 121–133.

Cigan, A. M., E. K. Pabich and T. F. Donahue, 1988 Mutational analysis of the *HIS4* translational initiator region in *Saccharomyces cerevisiae*. Mol. Cell. Biol. **8:** 2964–2975.

Conte, D., E. Barber, M. Banerjee, D. J. Garfinkel and M. J. Curcio, 1998 Posttranslational regulation of Ty1 retrotransposition by the MAP kinase, Fus 3. Mol. Cell. Biol. (in press).

Craigie, R., 1992 Hotspots and warm spots: integration specificity of retroelements. Trends Genet. **8:** 187–190.

Curcio, M. J., and D. J. Garfinkel, 1991 Single-step selection for Ty1 element retrotransposition. Proc. Natl. Acad. Sci. USA **88:** 936–940.

Curcio, M. J., and D. J. Garfinkel, 1992 Posttranslational control of Ty1 retrotransposition occurs at the level of protein processing. Mol. Cell. Biol. **12:** 2813–2825.

Curcio, M. J., and D. J. Garfinkel, 1994 Heterogenous functional Ty1 elements are abundant in the *Saccharomyces cerevisiae* genome. Genetics **136:** 1245–1259.

Curcio, M. J., and R. H. Morse, 1996 *Ty*ing together integration and chromatin. Trends Genet. **12:** 436–438.

Curcio, M. J., A. M. Hedge, J. D. Boeke and D. J. Garfinkel, 1990 Ty RNA levels determine the spectrum of retrotransposition events that activate gene expression in *Saccharomyces cerevisiae*. Mol. Gen. Genet. **220:** 213–221.

Devine, S. E., and J. D. Boeke, 1996 Integration of the yeast retrotransposon Ty1 is targeted to regions upstream of genes transcribed by RNA polymerase III. Genes Dev. **10:** 620–633.

Drake, J. W., 1970 *The Molecular Basis of Mutation*. Holden-Day, San Francisco.

Eichinger, D. J., and J. D. Boeke, 1988 The DNA intermediate in yeast Ty1 element transposition copurifies with virus-like particles: cell-free Ty1 transposition. Cell **54:** 955–966.

Eichinger, D. J., and J. D. Boeke, 1990 A specific terminal structure is required for Ty1 transposition. Genes Dev. **4:** 324–330.

Elder, R. T., E. Y. Loh and R. W. Davis, 1983 RNA from the yeast transposable element Ty1 has both ends in the direct repeats, a structure similar to retrovirus RNA. Proc. Natl. Acad. Sci. USA **80:** 2432–2436.

Errede, B., T. S. Cardillo, F. Sherman, E. Dubois, J. Deschamps *et al.*, 1980 Mating signals control expression of mutations resulting from insertion of a transposable repetitive element adjacent to diverse yeast genes. Cell **22:** 427–436.

Farabaugh, P. J., 1995 Post-transcriptional regulation of transposition by Ty retrotransposons of *Saccharomyces cerevisiae.* J. Biol. Chem. **270:** 10361–10364.

Farnet, C. M., and F. D. Bushman, 1997 HIV-1 cDNA integration: requirement of HMG I(Y) protein for function of preintegration complexes in vitro. Cell **88:** 483–492.

Feaver, W. J., J. Q. Svejstrup, L. Bardwell, A. J. Bardwell, S. Buratowski *et al.*, 1993 Dual roles of a multiprotein complex from *S. cerevisiae* in transcription and DNA repair. Cell **75:** 1379–1387.

Flavell, A. J., 1995 Retroelements, reverse transcriptase and evolution. Comp. Biochem. Physiol. B Biochem. Mol. Biol. **110:** 3–15.

Garfinkel, D. J., 1992 Retroelements in microorganisms, pp. 107–158 in *The Retroviridae,* edited by J. A. Levy. Plenum Press, New York.

Garfinkel, D. J., J. D. Boeke and G. R. Fink, 1985 Ty element transposition: reverse transcriptase and virus-like particles. Cell **42:** 507–517.

Garfinkel, D. J., A. M. Hedge, S. D. Youngren and T. D. Copeland, 1991 Proteolytic processing of pol-TYB proteins from the yeast retrotransposon Ty1. J. Virol. **65:** 4573–4581.

Goffeau, A., B. G. Barrell, H. Bussey, R. W. Davis, B. Dujon *et al.*, 1996 Life with 6000 genes. Science **274:** 563–567.

Gulyas, K. D., and T. F. Donahue, 1992 *SSL2,* a suppressor of a stem-loop mutation in the *HIS4* leader encodes the yeast homolog of human ERCC-3. Cell **69:** 1031–1042.

Guthrie, C., and G. R. Fink, 1991 *Guide to Yeast Genetics and Molecular Biology, Methods in Enzymology,* Vol. 194, Academic Press, Inc., San Diego.

Guzder, S. N., H. Qiu, C. H. Sommers, P. Sung, L. Prakash *et al.*, 1994a DNA repair gene *RAD3* of *S. cerevisiae* is essential for transcription by RNA polymerase II. Nature **367:** 91–94.

Guzder, S. N., P. Sung, V. Bailly, L. Prakash and S. Prakash, 1994b *RAD25* is a DNA helicase required for DNA repair and RNA polymerase II transcription. Nature **369:** 578–581.

Guzder, S. N., P. Sung, L. Prakash and S. Prakash, 1996 Nucleotide excision repair in yeast is mediated by sequential assembly of repair factors and not be a pre-assembled repairosome. J. Biol. Chem. **271:** 8903–8910.

Hoffman, C. S., and F. Winston, 1987 A ten-minute DNA preparation from yeast efficiently releases autonomous plasmids for transformation of *Escherichia coli.* Gene **57:** 267–272.

Ji, H., D. P. Moore, M. A. Blomberg, L. T. Braiterman, D. F. Voytas *et al.*, 1993 Hotspots for unselected Ty1 transposition events on yeast chromosome III are near tRNA genes and LTR sequences. Cell **73:** 1007–1018.

Kalpana, G. V., S. Marmon, W. Wang, G. R. Crabtree and S. P. Goff, 1994 Binding and stimulation of HIV-1 integrase by a human homolog of yeast transcription factor SNF5. Science **266:** 2002–2006.

Lawrence, C., 1994 The *RAD6* DNA Repair Pathway in *Saccharomyces cerevisiae:* What does it do, and how does it do it? BioEssays **16:** 253–258.

Lee, M. S., and R. Craigie, 1994 Protection of retroviral DNA from autointegration: involvement of a cellular factor. Proc. Natl. Acad. Sci. USA **91:** 9823–9827.

Lehmann, A. R., 1995 Nucleotide excision repair and the link with transcription. Trends Biochem. Sci. **20:** 402–405.

Liebman, S. W., and G. Newnam, 1993 A ubiquitin-conjugating enzyme, *RAD6,* affects the distribution of Ty1 retrotransposon integration positions. Genetics **133:** 499–508.

Manivasakam, P., S. C. Weber, J. McElver and R. H. Schiestl, 1995 Micro-homology mediated PCR targeting in *Saccharomyces cerevisiae.* Nucleic Acids Res. **23:** 2799–2800.

McClintock, B., 1984 The significances of responses of the genome to challenge. Science **226:** 792–801.

Miller, M. D., C. M. Farnet and F. D. Bushman, 1997 Human immunodeficiency virus type 1 preintegration complexes: studies of organization and composition. J. Virol. **71:** 5382–5390.

Montelone, B. A., M. F. Hoekstra and R. E. Malone, 1988 Spontaneous mitotic recombination in yeast: the hyper-recombinational *rem1* mutations are alleles of the *RAD3* gene. Genetics **119:** 289–301.

Mounkes, L. C., R. S. Jones, B. C. Liang, W. Gelbart and M. T. Fuller, 1992 A *Drosophila* model for xeroderma pigmentosum and Cockayne's syndrome: haywire encodes the fly homolog of *ERCC3,* a human excision repair gene. Cell **71:** 925–937.

Orphanides, G., T. Lagrange and D. Reinberg, 1996 The general transcription factors of RNA polymerase II. Genes Dev. **10:** 2657–2683.

Park, E., S. N. Guzder, M. H. Koken, I. Jaspers-Dekker, G. Weeda *et al.*, 1992 *RAD25* (*SSL2*), the yeast homolog of the human xeroderma pigmentosum group B DNA repair gene, is essential for viability. Proc. Natl. Acad. Sci. USA **89:** 11416–11420.

Pryciak, P. M., and H. E. Varmus, 1992 *Fv-1* restriction and its effects on murine leukemia virus integration *in vivo* and *in vitro.* J. Virol. **66:** 5959–5966.

Qiu, H., E. Park, L. Prakash and S. Prakash, 1993 The *Saccharomyces cerevisiae* DNA repair gene *RAD25* is required for transcription by RNA polymerase II. Genes Dev. **7:** 2161–2171.

Rattray, A. J., and L. S. Symington, 1994 Use of a chromosomal inverted repeat to demonstrate that the *RAD51* and *RAD52* genes of *Saccharomyces cerevisiae* have different roles in mitotic recombination. Genetics **138:** 587–595.

Rinckel, L. A., and D. J. Garfinkel, 1996 Influences of histone stoichiometry on the target site preference of retrotransposons Ty1 and Ty2 in *Saccharomyces cerevisiae.* Genetics **142:** 761–776.

Roberts, R. L., and G. R. Fink, 1994 Elements of a single MAP kinase cascade in *Saccharomyces cerevisiae* mediate two developmental programs in the same cell type: mating and invasive growth. Genes Dev. **8:** 2974–2985.

Rolfe, M., A. Spanos and G. Banks, 1986 Induction of yeast Ty element transcription by ultraviolet light. Nature **319:** 339–340.

Rose, M., M. J. Casadaban and D. Botstein, 1981 Yeast genes fused to beta-galactosidase in *Escherichia coli* can be expressed normally in yeast. Proc. Natl. Acad. Sci. USA **78:** 2460–2464.

Rose, M. D., P. Novick, J. H. Thomas, D. Botstein and G. R. Fink, 1987 A *Saccharomyces cerevisiae* genomic plasmid bank based on a centromere-containing shuttle vector. Gene **60:** 237–243.

Rose, M. D., F. Winston and P. Hieter, 1990 Hydroxylamine mutagenesis of plasmid DNA, p. 198 in *Methods in Yeast Genetics.* Cold Spring Harbor Laboratory Press, Cold Spring Harbor, NY.

Sambrook, J., E. Fritsch and T. Maniatis, 1989 *Molecular Cloning, a Laboratory Manual.* Cold Spring Harbor Laboratory Press, Cold Spring Harbor, NY.

Sandmeyer, S. B., L. J. Hansen and D. L. Chalker, 1990 Integration specificity of retrotransposons and retroviruses. Annu. Rev. Genet. **24:** 491–518.

Sharon, G., T. J. Burkett and D. J. Garfinkel, 1994 Homologous recombination of Ty1 element cDNA when integration is blocked. Mol. Cell. Biol. **14:** 6540–6551.

Sherman, F., G. R. Fink and J. B. Hicks, 1986 *Methods in Yeast Genetics.* Cold Spring Harbor Laboratory Press, Cold Spring Harbor, NY.

Sikorski, R. S., and P. Hieter, 1989 A system of shuttle vectors and yeast host strains designed for efficient manipulation of DNA in *Saccharomyces cerevisiae.* Genetics **122:** 19–27.

Smith, V., D. Botstein and P. O. Brown, 1995 Genetic footprinting: a genomic strategy for determining a gene's function given its sequence. Proc. Natl. Acad. Sci. USA **92:** 6479–6483.

Song, J. M., B. A. Montelone, W. Siede and E. C. Friedberg, 1990 Effects of multiple yeast rad3 mutant alleles on UV sensitivity, mutability, and mitotic recombination. J. Bacteriol. **172:** 6620–6630.

Struhl, K., D. T. Stinchcomb, S. Scherer and R. W. Davis, 1979 High-frequency transformation of yeast: autonomous replication of hybrid DNA molecules. Proc. Natl. Acad. Sci. USA **76:** 1035–1039.

Subramanya, H. S., L. E. Bird, J. A. Brannigan and D. B. Wigley, 1996 Crystal structure of a DExx box DNA helicase. Nature **384:** 379–383.

Sung, P., L. Prakash, S. Weber and S. Prakash, 1987 The *RAD3* gene of *Saccharomyces cerevisiae* encodes a DNA-dependent ATPase. Proc. Natl. Acad. Sci. USA **84:** 6045–6049.

Sung, P., S. N. Guzder, L. Prakash and S. Prakash, 1996 Reconstitution of TFIIH and requirement of its DNA helicase subunits, Rad3 and Rad25, in the incision step of nucleotide excision repair. J. Biol. Chem. **271:** 10821–10826.

Svejstrup, J. Q., Z. Wang, W. J. Feaver, X. Wu, D. A. Bushnell *et*

al., 1995 Different forms of TFIIH for transcription and DNA repair: holo-TFIIH and a nucleotide excision repairosome. Cell **80:** 21–28.

Svejstrup, J. Q., P. Vichi and J. M. Egly, 1996 The multiple roles of transcription/repair factor TFIIH. Trends Biochem. Sci. **21:** 346–350.

Sweder, K. S., and P. C. Hanawalt, 1994 The COOH terminus of suppressor of stem loop Ssl2/Rad25 in yeast is essential for overall genomic excision repair and transcription-coupled repair. J. Biol. Chem. **269:** 1852–1857.

Temin, H. M., 1985 Reverse transcription in the eukaryotic genome: retroviruses, pararetroviruses, retrotransposons, and retrotranscripts. Mol. Biol. Evol. **2:** 455–468.

Voytas, D. F., 1996 Retroelements in genome organization. Science **274:** 737–738.

Walker, J. E., M. Saraste, M. J. Runswick and N. J. Gay, 1982 Distantly related sequences in the alpha- and beta-subunits of ATP synthase, myosin, kinases and other ATP-requiring enzymes and a common nucleotide binding fold. EMBO J. **1:** 945–951.

Wang, Z., J. Q. Svejstrup, W. J. Feaver, X. Wu, R. D. Kornberg *et al.*, 1994 Transcription factor b (TFIIH) is required during nucleotide-excision repair in yeast. Nature **368:** 74–76.

Wang, Z., S. Buratowski, J. Q. Svejstrup, W. J. Feaver, X. Wu *et al.*, 1995 The yeast *TFB1* and *SSL1* genes, which encode subunits of transcription factor IIH, are required for nucleotide excision repair and RNA polymerase II transcription. Mol. Cell. Biol. **15:** 2288–2293.

Weeda, G., R. C. van Ham, W. Vermeulen, D. Bootsma, A. J. van der Eb *et al.*, 1990 A presumed DNA helicase encoded by ERCC-3 is involved in the human repair disorders xeroderma pigmentosum and Cockayne's syndrome. Cell **62:** 777–791.

Weeda, G., M. Rossignol, R. A. Fraser, G. S. Winkler, W. Vermeulen *et al.*, 1997 The XPB subunit of repair/transcription factor TFIIH directly interacts with SUG1, a subunit of the 26S proteasome and putative transcription factor. Nucleic Acids Res. **25:** 2274–2283.

Wessler, S. R., 1996 Turned on by stress. Plant retrotransposons. Curr. Biol. **6:** 959–961.

Wilke, C. M., S. H. Heidler, N. Brown and S. W. Liebman, 1989 Analysis of yeast retrotransposon Ty insertions at the *CAN1* locus. Genetics **123:** 655–665.

Winston, F., K. J. Durbin and G. R. Fink, 1984 The *SPT3* gene is required for normal transcription of Ty elements in *S. cerevisiae.* Cell **39:** 675–682.

Youngren, S. D., J. D. Boeke, N. J. Sanders and D. J. Garfinkel, 1988 Functional organization of the retrotransposon Ty from *Saccharomyces cerevisiae:* Ty protease is required for transposition. Mol. Cell. Biol. **8:** 1421–1431.

Communicating editor: A. G. Hinnebusch